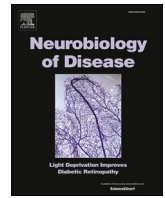




Since January 2020 Elsevier has created a COVID-19 resource centre with free information in English and Mandarin on the novel coronavirus COVID-19. The COVID-19 resource centre is hosted on Elsevier Connect, the company's public news and information website.

Elsevier hereby grants permission to make all its COVID-19-related research that is available on the COVID-19 resource centre - including this research content - immediately available in PubMed Central and other publicly funded repositories, such as the WHO COVID database with rights for unrestricted research re-use and analyses in any form or by any means with acknowledgement of the original source. These permissions are granted for free by Elsevier for as long as the COVID-19 resource centre remains active.



SARS-CoV-2 deregulates the vascular and immune functions of brain pericytes via Spike protein

Rayan Khaddaj-Mallat^{a,c}, Natija Aldib^{a,b,c}, Maxime Bernard^{a,c}, Anne-Sophie Paquette^{a,c}, Aymeric Ferreira^{b,d}, Sarah Lecordier^{a,c}, Armen Saghatelian^{b,c}, Louis Flamand^{a,e}, Ayman ElAli^{a,c,*}

^a Neuroscience Axis, Research Center of CHU de Québec - Université Laval, Québec City, QC, Canada

^b Research Center CERVO, Québec City, QC, Canada

^c Department of Psychiatry and Neuroscience, Faculty of Medicine, Université Laval, Québec City, QC, Canada

^d Department of Computer Science and Software Engineering, Université Laval, Québec City, QC, Canada

^e Department of Microbiology, Infectious Diseases and Immunology, Faculty of Medicine, Université Laval, Québec City, QC, Canada

ARTICLE INFO

Keywords:

COVID-19
SARS-CoV-2 S protein
Pericytes
Neurovascular interface
Cerebrovascular disorders
Inflammation
Myofibroblastic transition

ABSTRACT

Coronavirus disease 19 (COVID-19) is a respiratory illness caused by severe acute respiratory syndrome coronavirus-2 (SARS-CoV-2). COVID-19 pathogenesis causes vascular-mediated neurological disorders via elusive mechanisms. SARS-CoV-2 infects host cells via the binding of viral Spike (S) protein to transmembrane receptor, angiotensin-converting enzyme 2 (ACE2). Although brain pericytes were recently shown to abundantly express ACE2 at the neurovascular interface, their response to SARS-CoV-2 S protein is still to be elucidated. Using cell-based assays, we found that ACE2 expression in human brain vascular pericytes was increased upon S protein exposure. Pericytes exposed to S protein underwent profound phenotypic changes associated with an elongated and contracted morphology accompanied with an enhanced expression of contractile and myofibroblastic proteins, such as α -smooth muscle actin (α -SMA), fibronectin, collagen I, and neurogenic locus notch homolog protein-3 (NOTCH3). On the functional level, S protein exposure promoted the acquisition of calcium (Ca^{2+}) signature of contractile ensheathing pericytes characterized by highly regular oscillatory Ca^{2+} fluctuations. Furthermore, S protein induced lipid peroxidation, oxidative and nitrosative stress in pericytes as well as triggered an immune reaction translated by activation of nuclear factor-kappa-B (NF- κ B) signaling pathway, which was potentiated by hypoxia, a condition associated with vascular comorbidities that exacerbate COVID-19 pathogenesis. S protein exposure combined to hypoxia enhanced the production of pro-inflammatory cytokines involved in immune cell activation and trafficking, namely macrophage migration inhibitory factor (MIF). Using transgenic mice expressing the human ACE2 that recognizes S protein, we observed that the intranasal infection with SARS-CoV-2 rapidly induced hypoxic/ischemic-like pericyte reactivity in the brain of transgenic mice, accompanied with an increased vascular expression of ACE2. Moreover, we found that SARS-CoV-2 S protein accumulated in the intranasal cavity reached the brain of mice in which the nasal mucosa is deregulated. Collectively, these findings suggest that SARS-CoV-2 S protein impairs the vascular and immune regulatory functions of brain pericytes, which may account for vascular-mediated brain damage. Our study provides a better understanding for the mechanisms underlying cerebrovascular disorders in COVID-19, paving the way to develop new therapeutic interventions.

1. Introduction

The current COVID-19 pandemic has emerged as a respiratory disease caused by an infection with a novel coronavirus, SARS-CoV-2 (Zhou

et al., 2020). COVID-19 is causing an unprecedented worldwide socio-economic burden and is currently accounting for more than 250 million confirmed infection cases and 5 million deaths [<https://coronavirus.jhu.edu>]. Initial clinical observations have reported typical symptoms

* Corresponding author at: Neuroscience Axis (T2-33), Research Center of CHU de Québec-Université Laval, 2705 Laurier Boulevard, Québec City, QC G1V 4G2, Canada.

E-mail address: ayman.el-ali@crchudequebec.ulaval.ca (A. ElAli).

<https://doi.org/10.1016/j.nbd.2021.105561>

Received 15 June 2021; Received in revised form 9 November 2021; Accepted 11 November 2021

Available online 13 November 2021

0969-9961/© 2021 The Authors.

Published by Elsevier Inc.

This is an open access article under the CC BY-NC-ND license

(<http://creativecommons.org/licenses/by-nc-nd/4.0/>).

associated to an infection with respiratory viruses, such as fever and cough, as well as some atypical symptoms, including hyposmia, anosmia, headache, and diarrhea (Mao et al., 2020; Klok et al., 2020). An important proportion of infected individuals develop serious complications, such as severe respiratory distress, pulmonary pneumonia, heart injury, and sepsis (Mao et al., 2020; Klok et al., 2020). The clinical observations are increasingly reporting unexpected neurological symptoms associated to vascular-mediated disorders among which are cerebrovascular disorders including multifocal cerebral micro-occlusions and stroke (Mao et al., 2020; Klok et al., 2020). The clinical and epidemiological studies have unveiled an association between the presence of comorbid vascular conditions, such as obesity, hypertension and diabetes, and the risk to develop life-threatening complications (Richardson et al., 2020). The observed neurological disorders are often associated to an excessive inflammation, which comprises the “cytokine storm”, as well as coagulopathies and multifocal microvascular injuries (He et al., 2020). The accurate mechanisms underlying cerebrovascular disorders in COVID-19 are now under intensive investigations.

Infection of respiratory epithelial cells by SARS-CoV-2 is like the one observed with other coronaviruses, namely SARS-CoV-1 (Hoffmann et al., 2020; Ou et al., 2020). It occurs through the direct binding of viral Spike (S) protein to a host cell transmembrane receptor complex that facilitates its cleavage and the subsequent fusion of viral and cellular membranes, thus allowing viral RNA entry into host cells (Hoffmann et al., 2020; Ou et al., 2020). Recently, angiotensin-converting enzyme-2 (ACE2), an enzyme that plays a critical role in the renin-angiotensin system (RAS), has been identified as the main receptor for SARS-CoV-2 S protein (Ou et al., 2020; Lovren et al., 2008). Moreover, the transmembrane serine protease-2 (TMPRSS2) and cathepsin-B/L (CTSB/L) has been identified as the main proteases involved in S protein cleavage and processing by host cells (Hoffmann et al., 2020; Ou et al., 2020; Lovren et al., 2008). ACE2 high expression levels in respiratory epithelial cells accounts for the initial respiratory symptoms observed in COVID-19 (Hoffmann et al., 2020; Ou et al., 2020). Nonetheless, accumulating evidence is suggesting that the neurological symptoms related to COVID-19 cannot be solely attributed to the primary active respiratory infection (Klok et al., 2020; He et al., 2020). It has been previously shown that ACE2 is abundantly expressed in platelet-derived growth factor receptor (PDGFR) β^+ perivascular cells, which comprise mainly pericytes (He et al., 2020). Its expression was also observed, albeit at much lower extent, in other cells present at the neurovascular interface, such as endothelial cells, perivascular macrophages, fibroblasts and neuroglial cells (He et al., 2020). These findings suggest that SARS-CoV-2 infection of pericytes may be implicated in mediating microvasculature injury in COVID-19 (He et al., 2020). Brain pericytes are specialized cells that play essential roles in generating critical neurovascular functions that include blood-brain barrier (BBB) maintenance, and neurovascular coupling via cerebral blood flow (CBF) regulation (ElAli et al., 2014; Kisler et al., 2017; Armulik et al., 2011; Sweeney et al., 2019). Furthermore, pericytes were shown to possess immunoregulatory properties that include secretion of various inflammatory mediators at the neurovascular interface, as well as regulation of immune cell activation and infiltration into the brain parenchyma (ElAli et al., 2014; Török et al., 2021). Moreover, a population of PDGFR β^+ pericytes has been shown to contribute to the fibrotic reaction upon brain injuries by acquiring myofibroblast-like properties associated with an upregulation of stromal markers, including α -smooth muscle actin (α -SMA) and production of extracellular matrix proteins (Dias et al., 2021). Calcium (Ca) $^{2+}$ signaling has been shown to play key role in modulating the contractile activity of perivascular cells including pericytes, which in turn regulate CBF and vasomotion (Burdyga and Borysova, 2014; Halaidych et al., 2019; Hartmann et al., 2021). A recent report has demonstrated that brain pericytes have distinct signatures of Ca $^{2+}$ activity depending upon localization within the vascular tree and neuronal activity (Glück et al., 2021). For instance, ensheathing pericytes, which are located at the level of penetrating arterioles and pre-capillaries, have

been shown to exhibit highly regular oscillatory fluctuations like those of smooth muscle cells (SMC) and to possess an important contractile potential to regulate the CBF (Glück et al., 2021). On the other hand, capillary and venular pericytes, which are less efficient in regulating CBF, exhibited irregular Ca $^{2+}$ signals of different frequencies (Glück et al., 2021). Interestingly, deregulation of pericyte function is directly implicated in the pathobiology of cerebrovascular disorders (ElAli et al., 2014; Armulik et al., 2011; Sweeney et al., 2019; Török et al., 2021).

The emerging findings suggest that PDGFR β^+ pericytes constitute the main cell type at the neurovascular interface that could actively respond to SARS-CoV-2 infection (He et al., 2020; Wang et al., 2021). Based on these findings, an exciting “COVID-19-pericyte hypothesis” has been proposed as an attempt to outline the pathological links between SARS-CoV-2 infection and vascular-mediated neurological symptoms in COVID-19, especially in patients presenting vascular comorbid and risk factors (He et al., 2020; Bocci et al., 2021). As such, the mechanisms that mediate the effects of SARS-CoV-2 on ACE2 $^+$ pericytes is now under intensive investigations. Currently, it is proposed that the direct passage of SARS-CoV-2 viral particles through a dysfunctional endothelial barrier to actively infect ACE2 $^+$ pericytes accounts for microvascular injuries in COVID-19 (He et al., 2020). In this regard, recent reports have outlined the presence of SARS-CoV-2 viral proteins in the brainstem, which was not necessarily associated with the severity of neuropathological changes (Lee et al., 2021; Thakur et al., 2021; Matschke et al., 2020). Multifocal microvascular injuries were reported in the brain of patients infected with SARS-CoV-2 presenting mild to severe symptoms and who died later after viral infection resolution (Lee et al., 2021; Thakur et al., 2021; Matschke et al., 2020). The injury was associated to punctate hypointensities, corresponding to congested vasculature with surrounding areas of fibrinogen leakage, and areas of linear hypointensities, corresponding to microhemorrhages (Lee et al., 2021). In line with these evidence, global and focal hypoxic/ischemic zones associated to large and small infarcts, accompanied by microglial activation, were reported as well in the brain of COVID-19 patients who died later after hospitalization (Lee et al., 2021; Thakur et al., 2021; Matschke et al., 2020). As such, it is becoming critically important to better characterize the response of PDGFR β^+ pericytes to SARS-CoV-2, which may account for microvascular injuries in COVID-19. SARS-CoV-1 S protein, which shares approximately 76% of amino acid identity with SARS-CoV-2 S protein, has been previously shown to trigger an immune response in human peripheral blood monocytes and macrophages (Hoffmann et al., 2020; Dosch et al., 2009). Moreover, SARS-CoV-2 S protein has been recently shown to induce phenotypic changes in hematopoietic cells (Ropa et al., 2021). To our knowledge, the role of SARS-CoV-2 in modulating the function of brain pericytes via S protein remains largely explored. The current study aimed to investigate the reactivity of brain pericytes in response to SARS-CoV-2 S protein. Herein, we provide evidence indicating that SARS-CoV-2 deregulates the vascular and immune functions of brain pericytes via S protein, which may underlie the pathobiology of cerebrovascular disorders in COVID-19.

2. Materials and methods

2.1. Primary human cell cultures

Human vascular pericytes and human vascular smooth muscle cells (VSMCs) isolated from the brains of healthy individuals were purchased from ScienCell Research Laboratories (Carlsbad, CA, USA). Pericytes were maintained in pericyte growth medium (PGM) containing Dulbecco's modified eagle medium (DMEM) (Wisent Bioproducts, QC, Canada), 1% pericyte growth supplement (PGS) (ScienCell Research Laboratories), 2% fetal bovine serum (FBS) (Wisent Bioproducts), and 1% penicillin/streptomycin (Sigma-Aldrich, ON, Canada). VSMCs were maintained in smooth muscle cell medium (SMCM) containing Basal medium, 10% FBS, 1% smooth muscle cell growth supplement (SMCGS),

and 1% penicillin/streptomycin (ScienCell Research Laboratories). Cells were kept in a humidified incubator at 37 °C under 5% CO₂ and the culture medium was changed every 2–3 days. Pericytes were passed with 0.25% trypsin-EDTA and cells at passage 4–5 were used in this study. Cells were cultured either directly onto the plastic wells of multi-well plates for molecular experiments, or on poly-lysine-coated coverslips for immunocytochemical experiments. In all experiments, pericytes were seeded at a density of 50,000 cells per well. Upon reaching 75% confluency, cells were incubated overnight in PGM without FBS, to ensure synchronization in G1 phase. Pericytes were next treated afterwards for 6 or 24 h with the original SARS-CoV-2 S protein active trimer [Spike glycoprotein (COVID-19), R683A/R685A, poly-histidine-tagged (His-Tag), MALS verified] (ACROBiosystems, DE, USA) diluted in sterile ddH₂O at increasing concentrations; 5, 10 and 15 nM, which were calculated based on previous reports evaluating the role of SARS-CoV-1 S protein in activating inflammatory cells (Dorsch et al., 2009; Ropa et al., 2021). To assess the impact of hypoxia, cells were exposed to different hypoxic conditions, as described here below. Finally, to investigate the combined effects of hypoxia and S protein, cells were first exposed to hypoxic conditions for 48 h followed by an exposure to S protein at 10 nM for 24 h. These experimental conditions were chosen to ensure optimal stimulation of pericytes in absence of cell toxicity based on the dose response experiments. It has been shown that SARS-CoV-2 S protein is potentially recognized by human ACE2 and not by rodent ACE2, therefore, human brain pericytes were used in the study.

2.2. Hypoxia and oxygen/glucose deprivation induction

To investigate the response of pericytes to hypoxic/ischemic-like conditions, cells were subjected to either hypoxia or oxygen and glucose deprivation (OGD), as previously described (Jean LeBlanc et al., 2018; Jean LeBlanc et al., 2019). Hypoxia was induced by incubating cells at 37 °C in PGM under reduced oxygenation conditions (1% O₂, 5% CO₂) for different time points using a Modular Incubator Chamber (Billups-Rothenberg Inc., CA, USA). OGD was induced by incubating cells at 37 °C in a DMEM-glucose free medium (Multicell, Wisent, QC, Canada) in the presence of 1% oxygen (5% CO₂) overnight, as previously described. As control, cells obtained from the same passage were incubated at 37 °C in PGM under normal oxygenation conditions, i.e. normoxia. Cells were either harvested for protein extraction or fixed at room temperature with 2% paraformaldehyde (PFA) for immunocytochemical analysis.

2.3. Preparation of cell lysates

Pericytes and VSMCs were routinely grown into 6-well plates. Cells were maintained either under normoxic or hypoxic conditions in the presence of vehicle or S protein. At each time point, cells were washed twice in 1× cold sterile Dulbecco's phosphate-buffered saline (DPBS; Gibco®; 14190144) without Ca²⁺ and magnesium (Mg²⁺), and then lysated in ice-cold radio-immunoprecipitation assay (RIPA; Cell Signaling Technology; 9806) buffer supplemented with 1% protease inhibitor cocktail (Sigma-Aldrich) and 1% phosphatase inhibitor cocktail (Sigma-Aldrich), as specified before (Jean LeBlanc et al., 2019; Menet et al., 2020). Lysates were centrifuged at 14,000 rpm for 10 min at 4 °C. Supernatants were aliquoted into small Eppendorf tubes and snap frozen at –80 °C for further use. For the detection of phospho-NF-κB, lysates were prepared without centrifugation. Protein concentrations were determined using the bicinchoninic acid (BCA) assay (QuantiPro assay kit; Sigma-Aldrich).

2.4. Human cytokine and chemokine profiling

For each experimental condition, pericytes were harvested at 1 × 10⁷ cells/mL in RIPA lysis buffer. Lysates were gently mixed on a horizontal rotator at 2–8 °C for 30 min, centrifuged at 14,000 rpm for 5 min, and

the supernatants transferred to clean test tubes. Protein concentrations were assessed using BCA, and 200 µg of proteins were used per condition. The relative expression profile of 36 human cytokines and chemokines were evaluated using the Proteome Profiler Human Cytokine Array Kit (R&D Systems, ON, Canada; ARY005B). The experiment was performed according to the manufacturer's protocol, as previously described (Jean LeBlanc et al., 2018). Briefly, protein samples were mixed with biotinylated detection antibodies and then incubated with the array membrane which contains immobilized capture antibodies for the detection of a broad set of inflammatory cytokines and chemokines. Signals were visualized by streptavidin-HRP and chemiluminescent detection. Membranes were revealed and immediately digitized using Thermo Scientific myECL Imager (ThermoFisher Scientific, ON, Canada). Digitized blots were densitometrically analyzed with ImageJ software by measuring for each data spot the mean pixel intensity corrected for the background signal. Data were analyzed with mean values from duplicates and related to the mean of three internal control values on each membrane, as previously described (Jean LeBlanc et al., 2018).

2.5. Western blot analysis

Protein samples (25 µg) obtained from different experimental conditions were mixed with 2× sodium dodecyl sulfate (SDS)-loading buffer and heated for 10 min at 95 °C. Samples were subjected to 8%, 10%, or 12% SDS polyacrylamide gel electrophoresis (SDS-PAGE) using Mini-PROTEAN® Tetra Cell (Bio-Rad, CA, USA), as previously described (Jean LeBlanc et al., 2018). After migration, resolved protein bands were transferred onto Polyvinylidene Fluoride membranes (PVDF, 0.45 µm, EMD Millipore, ON, Canada) for 75 min on ice in a transfer buffer containing 25 mM Tris, 192 mM glycine, 0.1% SDS and 20% methanol. The PVDF membrane was rinsed three times with a 0.1 M Tris-buffered saline (TBS) solution containing 0.5% Tween-20 (TBS-Tween; Sigma-Aldrich) and blocked in TBS-Tween with 5% (*w/v*) skim milk for 45 min at room temperature. The PVDF membrane was then incubated overnight at 4 °C with different primary antibodies diluted at 1/1000 in TBS-T solution. The following primary antibodies were used; rabbit anti-ACE2 (Cell Signaling Technology, MA, USA; 4355), rabbit anti-α-SMA (Abcam, Cambridge, UK; ab5694), rabbit anti-fibronectin (Abcam; ab2413), rabbit anti-NOTCH3 (Abcam; ab23426), rabbit anti-NF-κB (p65) (Cell Signaling Technology; 8242), rabbit anti-phospho-NF-κB (p65) (Cell Signaling Technology; 3033), and mouse anti-β-actin (EMD Millipore; MAB1501). Following incubation with primary antibodies, membranes were washed with TBS-T for 3 × 5 min at room temperature, and then incubated for 2 h at room temperature in TBS-T containing the appropriate horseradish peroxidase (HRP)-conjugated secondary antibodies (Jackson ImmunoResearch, PA, USA) that were diluted 1/5000 in TBS-T and revealed by enhanced chemiluminescence plus (ECL) solution (Biorad Laboratories, ON, Canada). β-actin was used to ensure equal protein loading. Blots were revealed and immediately digitized using Thermo Scientific myECL Imager (ThermoFisher Scientific). Digitized blots were analyzed with ImageJ software, corrected for protein loading by means of β-actin, and expressed as relative values. In several experiments, the same membranes were used to probe different proteins by using different primary antibody; therefore, the same β-actin was used for correction and illustration.

2.6. F-actin staining

Brain pericytes were plated onto poly-lysine coated coverslips at different conditions, as mentioned previously. Cells were washed with 1× DPBS and fixed with 2% PFA for 5 min at room temperature. Cells were then rinsed once with 1× DPBS and permeabilized with 0.3% Triton X-100 in 1× DPBS for 10 min at room temperature. Next, cells were incubated with Alexa Fluor® 546 phalloidin diluted at 1/1000 in 0.1% Triton X-100 for 30 min at room temperature, as previously described (Jean LeBlanc et al., 2018). Stained cells were incubated with

DAPI (ThermoFisher Scientific) diluted at 1/20000 for few seconds at room temperature, and then mounted onto Superfrost® micro-slides with Fluoromount® anti-fade medium (Electron Microscopy Science, PA, USA). Epifluorescence images were taken using Axio Observer microscope equipped with Apotome.2 module, and Axiocam 503 monochrome camera, and were processed using ZEN Imaging Software (Carl Zeiss Canada, ON, Canada).

2.7. Immunocytochemical analysis

Pericytes were plated onto poly-lysine coated coverslips at different conditions, as mentioned previously (Menet et al., 2020). Cells were washed with 1× DPBS and fixed with 2% PFA for 5 min at room temperature, and then incubated for 1 h in a permeabilization/blocking solution containing 10% normal goat serum (NGS), 1% bovine serum albumin (BSA), 0.3% Triton X-100 in PBS. Next, cells were incubated over night at 4 °C with different primary antibodies diluted in 1% BSA, 0.2% Triton X-100 in 0.1 M PBS. The following primary antibodies were used; mouse anti- α -SMA Cy3-conjugated (Sigma-Aldrich; C6198; 1/250), rabbit anti-fibronectin (Abcam; ab18723; 1/250), rabbit anti-NOTCH3 (Abcam; ab23426; 1/250), rabbit anti-collagen I (Abcam; ab34710; 1/200), and mouse anti-ACE2 (Cell Signaling Technology; 15,983; 1/200). Afterwards, cells were rinsed in 0.1 M PBS, followed by a 2-h incubation with the appropriate secondary antibodies; Cy3 AffiniPure goat anti-mouse IgG (H + L) (Jackson ImmunoResearch), or Cy5 AffiniPure goat anti-rabbit IgG (H + L) (Jackson ImmunoResearch). Immunolabelled cells were incubated with DAPI (ThermoFisher Scientific) diluted at 1/20000 for few seconds at room temperature, and then mounted onto Superfrost® micro-slides with Fluoromount® anti-fade medium (Electron Microscopy Science). Epifluorescence images were taken using Axio Observer microscope equipped with Apotome.2 module, and Axiocam 503 monochrome camera, and were processed using ZEN Imaging Software (Carl Zeiss Canada).

2.8. Cell shape and morphology analysis

Cell circularity constitutes a morphological parameter that allows assessment of cell spreading, which is indicative whether cells are relaxed or contracted (Alisson-Silva et al., 2013; Padhi et al., 2020). A circularity index was computed using ImageJ software by applying the following formula: $4\pi(A)/(P)^2$, where A = area and P = perimeter. A circularity index from 0 at 1, where a value = 0 is related to elongated shape and value = 1 to a circular morphology. Cell perimeter is a morphology parameter that depends upon the size and shape of cells during spreading. It increases when small cells become large and round, and when round cells change shape without increasing their surface area. Cell body size parameter reflects the size of cell soma, which is reduced in contracted cells. Living cells without staining were used to avoid altering cell structure and representative images were captured using Axio Observer microscope equipped with a live imaging module (Carl Zeiss Canada). Analysis was achieved by delineating the outermost profile of cells to measure the average of contour and area in randomly acquired images. The analysis of each morphological parameter was performed in randomly selected 10 to 12 vehicle- and S protein-treated cells per image for a total of 3 images per well representing each of the experimental conditions.

2.9. Intracellular Ca^{2+} imaging and analysis

To assess spontaneous Ca^{2+} activity in human brain vascular pericytes, cells were treated with either S protein at 10 nM or vehicle for 4 h, were further incubated at the last hour with 2 μ M of Cal-590™ AM (AAT Bioquest, CA, USA) in a humidified incubator at 37 °C under 5% CO₂. Cal-590™ AM is a membrane-permeable organic dye that allows detection of intracellular Ca^{2+} fluctuations (Tischbirek et al., 2017). After incubation, the culture dish was transferred on the stage of a laser

scan confocal microscope (LSM 700, Carl Zeiss Canada) equipped with an incubation chamber allowing to maintain the temperature at 37 °C and CO₂ at 5%. Images were acquired every 10 s for 20 min and the recorded videos were analyzed using a custom-written script (Ropa et al., 2021) in MATLAB (MathWorks). Briefly, regions of interests (ROI) s were traced around the cell bodies and the fluorescence intensity in each ROI and for each time point was extracted. Ca^{2+} activity was calculated as relative changes in the percentage of $\Delta F/F = (F - F_{back})/F_{back}$, where F is the Cal-590™ AM intensity in the ROI and F_{back} is the background signal taken in a “cell-free” region of the imaging field. Analysis of spontaneous Ca^{2+} activity was performed used a multiple threshold algorithm (Gengatharan et al., 2021; Malvaut et al., 2017). Briefly, mean standard deviation (SD) of Ca^{2+} trace for each cell was first calculated, and all peaks with an amplitude greater than 1.5 times the SD were measured. These peaks were then removed from the Ca^{2+} traces, and the mean SD of Ca^{2+} trace was re-calculated to depict events greater than 1.5 times the new SD. This procedure allowed us to depict all Ca^{2+} events regardless of their amplitudes. Ca^{2+} frequency was calculated as the number of peaks over video duration, whereas synchronization was calculated as the average number of cells per each time point showing simultaneous Ca^{2+} fluctuations. The statistical analysis was performed in a total number of 7 videos collected from 4 wells for 371 cells in total in vehicle-treated pericytes, and 6 videos collected from 4 wells for 382 cells in total in S protein-treated pericytes.

2.10. XTT cell viability assay

The viability of pericytes and VSMCs was assessed using the 2,3-bis-(2-methoxy-4-nitro-5-sulphophenyl)-2H-tetrazolium-5-carboxanilide (XTT) assay according to the manufacturer’s procedure (Cell Signaling Technology; 9095). Cells were plated at the appropriate concentration in 96-well plates under different experimental conditions. One hundred μ L of cell culture medium was incubated with 50 μ L of XTT detection solution for 3 h at 37 °C. Cell viability was determined by reading absorbance at 450 nm using a microtiter plate reader (SpectraMax 340PC, Molecular Devices, CA, USA), and analyzed using SOFTmax Pro3.1.1 software, as previously described (Jean LeBlanc et al., 2018).

2.11. TBARS assay

Oxidative stress leads to lipid peroxidation resulting in the formation of malondialdehyde (MDA), which can be measured as thiobarbituric acid reactive substances (TBARS). As such, TBARS assay (R&D Systems; KGE013) was used to assess oxidative stress in pericytes under different experimental conditions, as previously described (Doepfner et al., 2012). Cells were plated in 6-well plates (BD Falcon®, BD, ON, Canada). Upon treatments, cells were resuspended at 1×10^6 cells/mL in RIPA buffer, with a gentle agitation for 30 min at 4 °C. Cell lysates were stored at -20 °C without centrifugation prior to use. The experiment was performed according to the manufacturer’s protocol. Briefly, TBARS generated in the assay which is proportional to cell peroxidation and oxidation in the sample is quantified by measuring the absorbance at wavelength 532 nm using a microtiter plate reader (SpectraMax 340PC, Molecular Devices), and analyzed using SOFTmax Pro3.1.1 software.

2.12. Cellular ROS/RNS assay

Real time reactive oxygen and/or nitrogen species (ROS/RNS) production was monitored in pericytes exposed to various experimental conditions by using the cellular ROS/RNS assay (Abcam, ab139473). The assay was conducted following manufacturer’s recommendation. Briefly, cells were incubated with mixture of three different fluorescent dye reagents that allow the simultaneous detection of nitric oxide (NO), total ROS, and superoxide. Standard green (Ex/Em = 490/525 nm), orange (Ex/Em = 550/620 nm), and red (Ex/Em = 650/670 nm) fluorescence was detected using Axio Observer microscope equipped

Apotome.2 module, and AxioCam 503 monochrome camera, and were processed using ZEN Imaging Software (Carl Zeiss Canada). Analysis of fluorescence intensity was performed using ImageJ software. Fluorescence images were separately acquired for each of the fluorophore to eliminate the crosstalk between the different fluorophores used. For each experimental condition, at least 14 to 15 cells per well of 12-well plates were randomly selected. Nuclear (total ROS and superoxide) and cytoplasmic (NO) structures were delineated and the fluorescence intensity in each structure was quantified to generate mean values that were analyzed.

2.13. Animal experiments

All animal experiments were performed under biosafety level 3 (BSL) confinement and according to the Canadian Council on Animal Care guidelines, as administered by the Université Laval Animal Welfare Committee. Mice were housed and acclimated to standard laboratory conditions (12-h light/dark cycle, lights on at 7:00 AM and off at 7:00 PM) with free access to chow and water. For SARS-CoV-2 infection experiments, adult female heterozygous K18-hACE2 transgenic mice (B6.Cg-Tg(K18-ACE2)2Prlmn/J) expressing the human ACE2 were used. These humanized hACE2 transgenic mice have been shown to recapitulate non-severe and severe COVID-19 pathologies in response to infectious dose of SARS-CoV-2 (Winkler et al., 2020; Oladunni et al., 2020). The heterozygous mice were obtained by crossbreeding homozygous K18 ACE2 mice with C57BL6/J mice. Mice were infected through the intranasal delivery of 25 μ L of 0.9% NaCl solution containing 4.5×10^4 TCID₅₀ of SARS-CoV-2. Mice were euthanized 4 days post infection via sedation with ketamine/xylazine (100/10mg/kg) and transcardiac perfusion with 0.1 M PBS. Brains were removed and a portion of the frontal lobe was used for RNA extraction to confirm SARS-CoV-2 viral presence by RT-qPCR. The remaining brains were post-fixed for 24 h in 4% PFA. For ischemic stroke experiments, adult male and female C57BL6/J mice were subjected to transient middle cerebral artery occlusion (MCAo) using the intraluminal filament technique as described (Jean LeBlanc et al., 2018). Briefly, mice were anaesthetized under 1.5% isoflurane (95% O₂) and body temperature was maintained between 36 °C and 37 °C using a feedback-controlled heating system (Harvard Apparatus, QC, Canada) throughout surgery. After a midline neck incision, the left common and external carotid arteries were isolated under a microscope and ligated. A microvascular clip was placed on the internal carotid artery and a 7–0 silicon-coated nylon monofilament (Doccol Corporation, MA, USA) was directed through the internal carotid artery until the origin of MCA. The monofilament was left in place for 30 min and then withdrawn. During the experiment, laser Doppler flow (LDF) was monitored using a flexible fiber-optic probe (OMEGAFLO, OMEGAWAVE INC., Tokyo, Japan) attached to the skull overlying the core of the MCA territory. Mice were euthanized 3 days after MCAo via sedation with ketamine/xylazine and transcardiac perfusion with 0.1 M PBS. Brains were removed and post-fixed for 24 h in 4% PFA.

2.14. His-tag protein ELISA

We used in our experiments the original active trimer of SARS-CoV-2 S protein, which is poly-histidine-tagged (His-Tag). In sub-group of wildtype mice, a total of 4 μ g of S protein diluted in 12 μ L sterile ddH₂O containing hyaluronidase (100 UI; Sigma-Aldrich) were infused into the intranasal cavity of mice, which were euthanized 24 h after infusion. Brains were removed, dissected and then different regions homogenized to quantify S protein, which is poly-histidine-tagged (His-Tag). The levels of S protein in different brain regions upon its intranasal infusion were measured using His-Tag protein ELISA kit that allows detection and quantification of poly-histidine-tagged proteins in a biological sample (Cell Biolabs Inc., CA, USA). The experimental procedure was performed as recommended by the manufacturer's instructions.

Absorbance was obtained using a microtiter plate reader (SpectraMax 340PC, Molecular Devices), and analyzed using SOFTmax Pro3.1.1 software (Molecular Devices).

2.15. Immunohistochemical analysis

Mice were sacrificed via a transcardiac perfusion with ice-cold 0.9% NaCl solution followed by post-fixation with 4% PFA (Jean LeBlanc et al., 2018; Jean LeBlanc et al., 2019; Menet et al., 2020). Brains were next cut on microtome into 25 μ m coronal sections that were kept in an anti-freeze solution (30% glycerol, 30% ethylene glycol in 0.9% NaCl, phosphate buffer (PB)) at -20 °C for further use. Free floating brain sections were rinsed with potassium phosphate-buffered saline (KPBS) (Sigma-Aldrich) and blocked for 45 min at room temperature in a permeabilization/blocking solution containing 4% NGS, 1% BSA (Sigma-Aldrich), and 1% triton X-100 in KPBS. Brain sections were then incubated with overnight at 4 °C with different primary antibodies at various dilution conditions in the permeabilization/blocking solution. The following primary antibodies were used; rabbit anti-PDGFR β (Abcam; ab32570; 1/250), goat anti-ACE2 (R&D systems; AF3437; 1/200), rabbit anti-fibronectin (Abcam; ab18723; 1/250), and rabbit anti-desmin (Abcam; ab15200; 1/500). The next day, brain sections were washed with KPBS and then incubated for 2 h at room temperature in the dark with either a secondary antibody donkey anti-goat Alexa Fluor 647® (Jackson ImmunoResearch) or donkey anti-rabbit Alexa Fluor 488® (Jackson ImmunoResearch) diluted 1/1000 in KPBS. Free-floating brain sections were mounted onto SuperFrost slides (Fisher Scientific) and coverslipped with Fluoromount® anti-fade medium (Electron Microscopy Science). Image acquisition was performed using a Zeiss LSM800 confocal microscope supported by ZEN Imaging Software (Carl Zeiss Canada).

2.16. Statistical analysis

Results are expressed as mean \pm standard error of the mean (SEM). For comparisons between two groups, unpaired two-tailed Student's *t*-test was used. For multiple comparisons, one-way analysis of variance (ANOVA) followed by Bonferroni's post-hoc test was used. For *in vivo* experiments, a violin plot outlining frequency distribution was used. Data normality distribution was assessed using Shapiro-Wilk test. *P*-values <0.05 were considered significant. All statistical analyses were performed using GraphPad Prism Version 9 for Mac (GraphPad Software, CA, USA).

3. Results

3.1. ACE2 expression in brain pericytes dynamically respond to S protein exposure

It has been recently demonstrated that within the neurovascular interface, pericytes specifically express ACE2 (He et al., 2020; Bocci et al., 2021), outlining their potential susceptibility to SARS-CoV-2 infection. However, the dynamics of ACE2 expression in pericytes upon exposure to S protein remains unknown. Here we show that S protein dose dependently increased ACE2 expression in brain pericytes as early as 6 h upon stimulation (Fig. 1A), peaking at 24 h after stimulation at the concentration of 10 nM, (Fig. 1B). Our data indicate that at higher concentrations (15 nM), S protein affected cell viability as early as 6 h after stimulation, assessed by XTT absorbance, which indicates that cells are metabolically active (Fig. 1C). This effect was maintained up to 24 h after stimulation (Fig. 1D). These results indicate that S protein increases ACE2 expression in brain pericytes, and thereby potentially affects cell responsiveness.

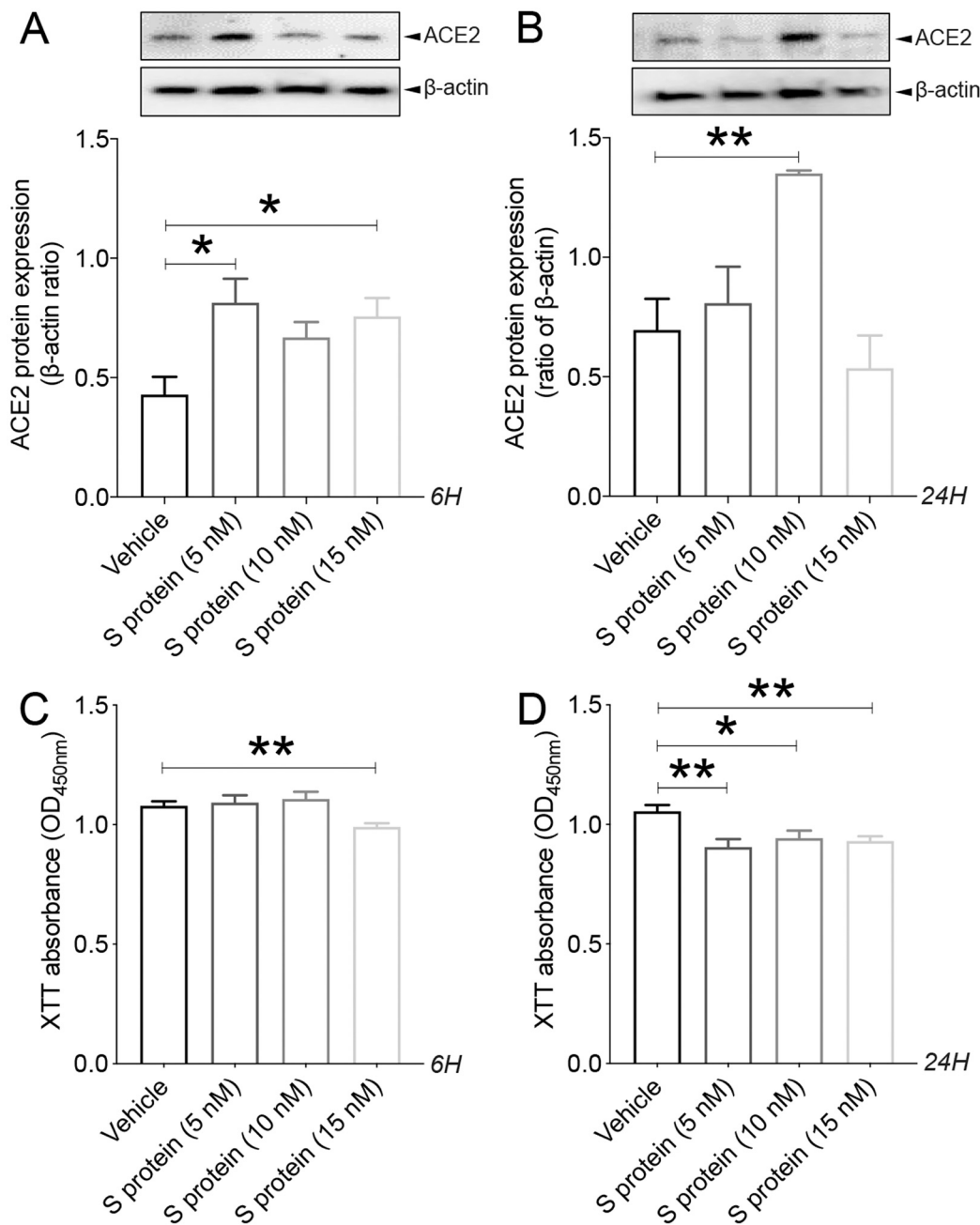


Fig. 1. S protein increases ACE2 expression in pericytes in a dose- and time-dependent manner. A) Western blot analysis shows that ACE2 expression in human brain vascular pericytes rapidly increases 6 h after exposure to 5 nM of S protein, reaching a peak at 15 nM. B) Western blot analysis shows that ACE2 expression in brain pericytes remains elevated 24 h after exposure to 10 nM of S protein compared to vehicle. C) XTT cell viability assay shows that exposure to 15 nM of S protein for 6 h attenuates the survival of brain pericytes. D) XTT cell viability assay shows that prolonged exposure to S protein for 24 h further attenuates the survival of brain pericytes. Data are mean \pm SEM ($n = 3$ independent experiments/ condition; XTT cell viability assay $n = 12$ wells/ condition). * $P < 0.05$ / ** $P < 0.01$ compared with vehicle-treated pericytes (two-tailed unpaired t -test). Vehicle, ddH₂O; 6H, 6 hours; 24H, 24 hours; XTT, 2/3-bis-(2-methoxy-4-nitro-5-sulphophenyl)-2H-tetrazolium-5-carboxanilide.

3.2. S protein induces pericyte contractile and myofibrogenic transition

Brain pericytes have been shown to acquire contractile and myofibroblast-like phenotypes under various pathological conditions, impairing brain perfusion and tissue regeneration (Dias et al., 2021; Yemisci et al., 2009; Fernández-Klett et al., 2013). The impact of S protein exposure on the expression of key contractile and fibrotic markers in brain pericytes remains to be elucidated. Here we demonstrated that S protein dose-dependently promoted the formation of highly dense actin filaments 6 h after stimulation and the adoption of contracted cell soma with increased protrusions and ramifications 24 h later (Fig. 2A). Next, we demonstrated that S protein at 10 nM induced the expression of α -SMA, a contractile protein implicated in pericyte-mediated vascular constriction (Yemisci et al., 2009), as early as 6 h after stimulation (Fig. 2B), which was further transiently increased 24 h after stimulation at 10 and 15 nM (Fig. 2C, D). Similarly, S protein at 10

nM triggered the expression of fibronectin, a major extracellular protein involved in the fibrotic response (Fernández-Klett et al., 2013; Laredo et al., 2019), as early as 6 h after stimulation (Fig. 3A), which was potentiated at 10 and 15 nM 24 h after stimulation (Fig. 3B, C). Additionally, we found that S protein stimulation for 6 h had little effects on the expression of NOTCH3, is involved in vascular degeneration via accumulation of its extracellular domain (ECD) in perivascular cells (Ghosh et al., 2015) (Fig. 3D), whereas its expression significantly increased following a stimulation for 24 h at 10 and 15 nM (Fig. 3E, F). The results suggest that S protein stimulates the pathological contractile and myofibrogenic potential of brain pericytes.

3.3. Pericytes adopt traits of contracted cells upon S protein exposure

Cell shape and morphology are associated with the phenotypic changes. Indeed, it was demonstrated that changes in cell morphology

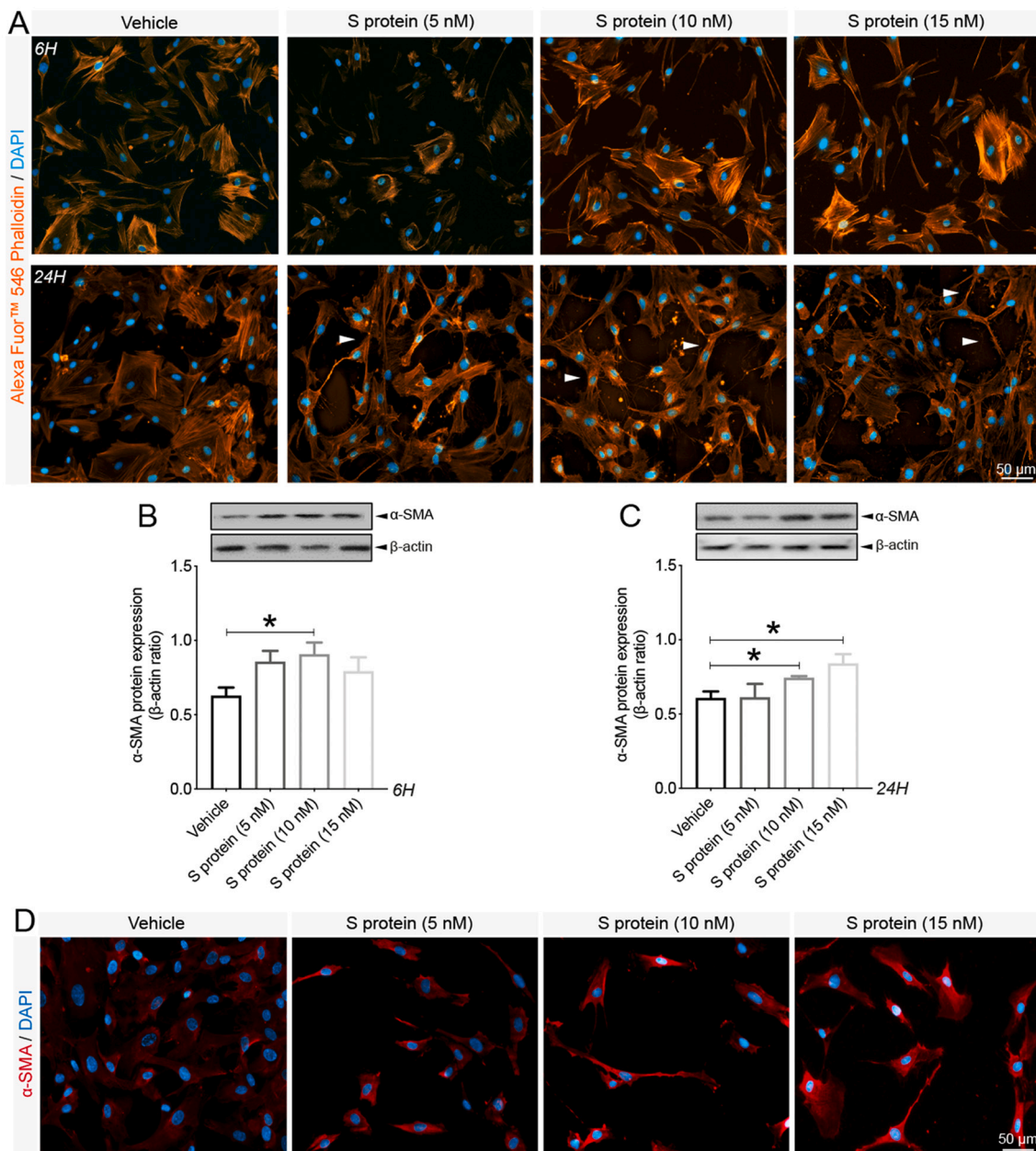


Fig. 2. Pericytes exhibit contractile phenotype upon S protein exposure. A) Representative images of F-actin staining using Alexa Fluor®546 phalloidin shows that the morphology of human brain vascular pericytes is disrupted (white arrowheads) upon exposure to S protein for 6 h and 24 h. B) Western blot analysis shows that expression of the contractile protein α -SMA increases in brain pericytes after exposure to 10 nM of S protein for 6 h. C) Western blot analysis shows that α -SMA expression in brain pericytes remains increased 24 h after exposure to 10 and 15 nM of S protein. D) Representative images of immunofluorescence staining that illustrate the expression pattern of α -SMA in brain pericytes in a dose-dependent manner upon exposure to S protein for 24 h. Data are mean \pm SEM ($n = 3$ independent experiments/ condition). * $P < 0.05$ compared with vehicle-treated pericytes (two-tailed unpaired t -test). Vehicle, ddH₂O; 6H, 6 hours; 24H, 24 hours.

correlated with changes in cell circularity, motility, and contraction of various cell types (Alisson-Silva et al., 2013; Padhi et al., 2020). To assess the putative effect of S protein on cell morphology parameters, brain pericytes were exposed for 24 h to different increasing S protein doses of 5 nM, 10 nM and 15 nM, and brightfield images were collected from living cells without fixation (Fig. 4A). S protein reduced cell circularity index of brain pericytes in a dose-dependent manner (Fig. 4B, C), indicative of the acquisition of an elongated shape. Moreover, exposure of brain pericytes to S protein decreased cell perimeter (Fig. 4D) as well as reduced cell body size (Fig. 4E) in a dose-dependent manner, which is reflected by a narrow cell soma. These results suggest that the prolonged exposure to S protein promote the transition of brain pericytes from a circular-like morphology associated to relaxed cells,

towards an elongated morphology associated to contractile cells.

3.4. VSMCs are minimally affected by S protein exposure

Brain VSMCs are located at brain arteries, possess higher contractility rate, and have been shown to respectively express PDGFR β and ACE2 (He et al., 2020). Nonetheless, SARS-CoV-2 S protein impact on VSMCs in response to S protein exposure remains unknown. As such, we assessed here the response of VSMCs to the prolonged exposure of S protein at different increasing doses of 5 nM, 10 nM and 15 nM. We found out that the protein expression of ACE2 (Fig. 5A, B) and α -SMA (Fig. 5A, C) remained unchanged in VSMCs 24 h after S protein exposure. Furthermore, analysis of cell shape and morphology (Fig. 5D)

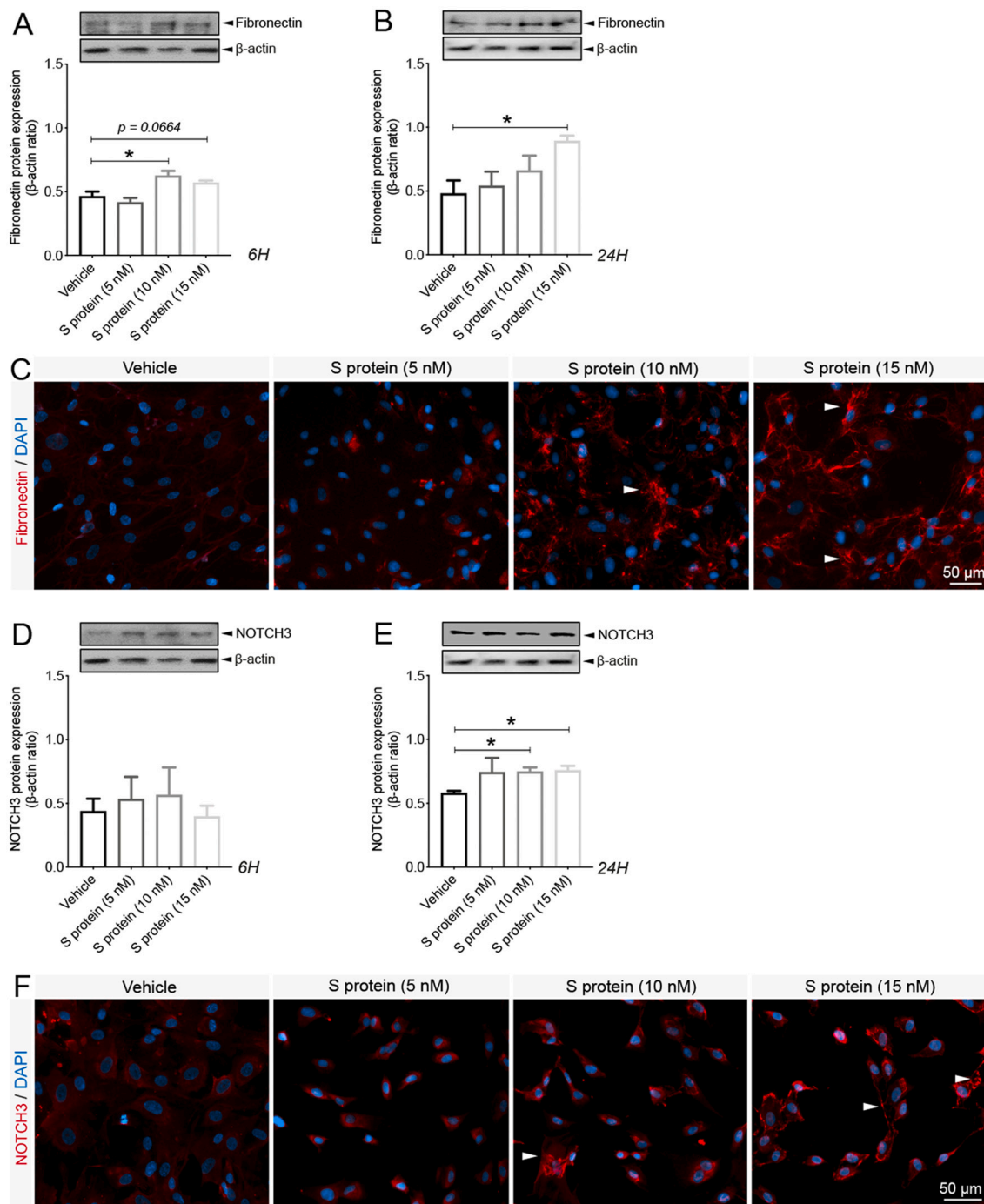


Fig. 3. S protein induces the expression of myofibrogenic markers in pericytes. A) Western blot analysis shows that expression of the pro-fibrotic protein fibronectin in human brain vascular pericytes is induced upon S protein exposure at 10 nM for 6 h. B) Western blot analysis shows that fibronectin expression in brain pericytes continues to increase after S protein exposure at 15 nM for 24 h. C) Representative images of immunofluorescence staining that illustrate the expression pattern of fibronectin in brain pericytes in a dose-dependent manner upon exposure to S protein for 24 h. D) Western blot analysis shows that expression of the fibrogenic protein NOTCH3 in brain pericytes remains unchanged after S protein exposure for 6 h, despite slight statistically non-significant increase at 5 and 10 nM. E) Western blot analysis shows that NOTCH3 expression in brain pericytes increases upon exposure to 10 and 15 nM S protein for 24 h. F) Representative images of staining that illustrates NOTCH3 expression pattern in brain pericytes in a dose-dependent manner upon exposure to S protein for 24 h, outlining a possible aggregation at the cell membrane in response to an elevated dose of S protein at 15 nM (white arrowheads). Data are mean \pm SEM ($n = 3$ independent experiments/condition). * $P < 0.05$ compared with vehicle-treated pericytes (two-tailed unpaired t-test). Vehicle, ddH₂O; 6H, 6 hours; 24H, 24 hours.

indicated that S protein exposure increased the cell circularity index (Fig. 5E), indicative of the presence of a large non-elongated shape. On the other hand, S protein exposure decreased the cell perimeter (Fig. 5F) and reduced the cell body shape (Fig. 5G) only at the higher concentration of 15 nM. The XTT assay indicated that S protein prolonged exposure did not affect cell viability (Fig. 5H) at any of the

concentrations assessed. These results suggest that S protein did not affect brain VSMCs despite their expression for ACE2, outlining higher resistance or resilience of the cells when compared to pericytes.

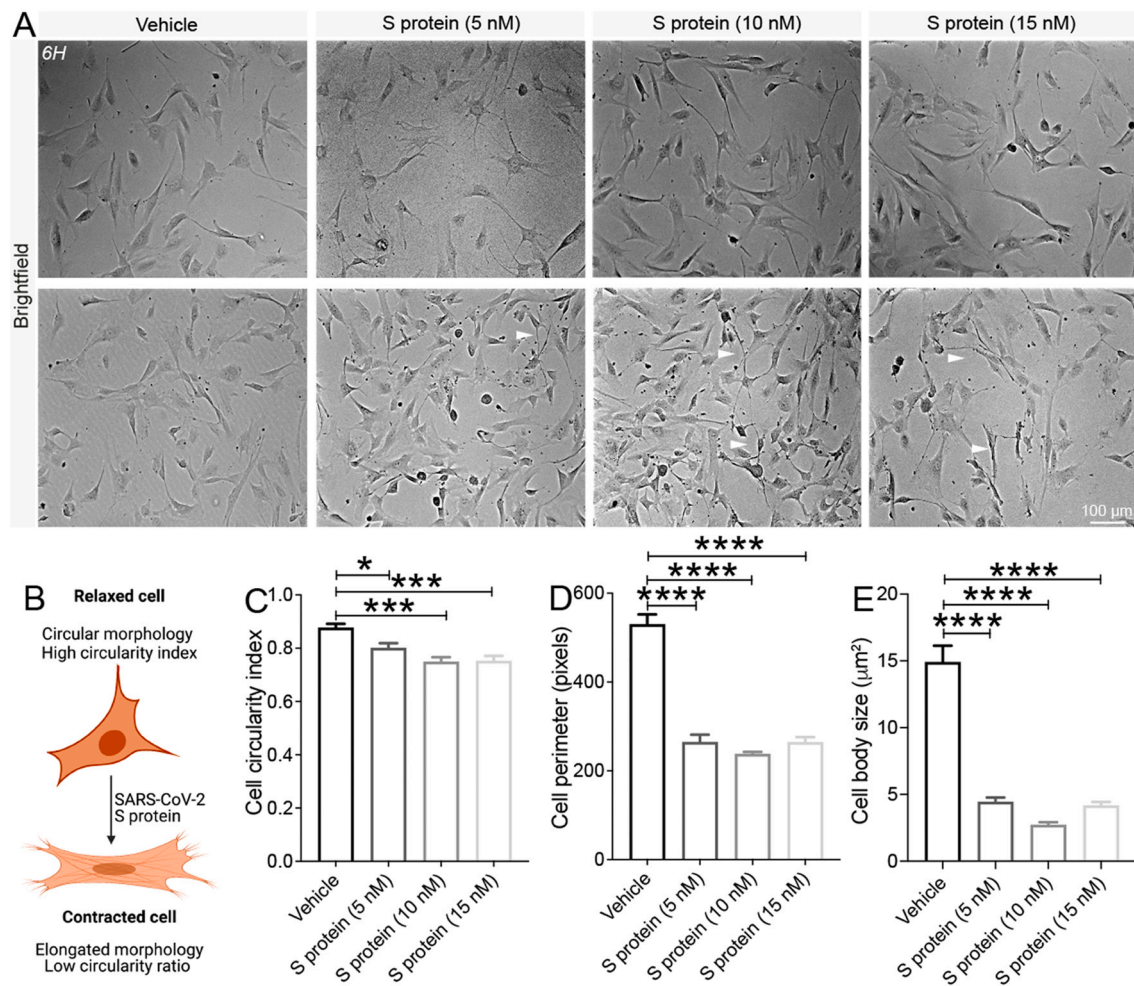


Fig. 4. Pericytes adopt an elongated and contracted shape upon S protein exposure. A) Representative brightfield images of living cells shows that human brain vascular pericytes exhibit an elongated morphology (white arrowheads) upon exposure to S protein for 24 h. B) A scheme illustrating the correlation between cell circularity index and contraction, where a reduced circularity index translates the acquisition of an elongated and contracted cellular morphology. Morphological analysis shows that the C) cell circularity index, D) cell perimeter, and E) cell body size (soma) decreases in brain pericytes exposed to S protein for 24 h in a dose-dependent manner. Data are mean \pm SEM (n = randomly selected 10 to 12 vehicle- and S protein-treated cells per image for a total of 3 images per experimental condition). * P < 0.05/ *** P < 0.001/ **** P < 0.0001 compared with vehicle-treated pericytes (two-tailed unpaired t-test). Vehicle, ddH₂O.

3.5. S protein modulates Ca²⁺ signaling in brain pericytes

It has been recently shown that brain pericytes have distinct Ca²⁺ signatures, which reflects specific contractile properties of different populations of pericytes depending upon their localization at the vascular tree (Glück et al., 2021). It remains however unknown whether protein S affects Ca²⁺ signaling dynamics in brain pericytes. To address this issue, we incubated human brain vascular pericytes with S protein for 4 h with a Ca²⁺-sensitive organic indicator Cal-590™ AM and performed time-lapse Ca²⁺ imaging (Fig. 6A; Supplementary video 1 [vehicle-treated pericytes]; Supplementary video 2 [S protein-treated pericytes]). Based on Ca²⁺ signature (Oladunni et al., 2020), we observed the presence of 4 distinct brain pericyte populations, which included ensheathing pericytes, capillary pericytes, venule pericytes, and an undetermined pericyte population (Fig. 6B). Interestingly, S protein exposure induced a Ca²⁺ oscillatory activity specific to ensheathing pericytes. Indeed, S protein exposure induced a major shift towards the Ca²⁺ signature of ensheathing pericytes that possess high contractility potential with highly regular oscillatory Ca²⁺ fluctuations (Fig. 6B), and disappearance of venular pericytes, which do not possess a contractile potential (Fig. 6C). Analysis of overall Ca²⁺ signals indicated that S protein induced an oscillatory activity in brain pericytes without affecting the amplitude of Ca²⁺ events (11.6 for control vs 11.9 for S

protein) (Fig. 6D). Importantly, S protein induced a 2-fold increase in the frequency (3.1 mHz and 6.7 mHz for control and S protein, respectively) (Figs. 6E) and the oscillatory Ca²⁺ activity resulted in an increased synchronized activity (Figs. 6F). These results indicate that S protein potently modulate Ca²⁺ signaling potentially associated to a transition towards a contractile phenotype of ensheathing pericytes.

3.6. ACE2 expression in brain pericyte is modulated by hypoxic conditions

Vascular comorbidities and risk factors have been shown to exacerbate COVID-19 pathogenesis (Fraiman et al., 2020; Ellul et al., 2020). These conditions are often associated to tissue hypoxia/ischemia caused by vascular dysfunction (Kisler et al., 2017). Yet, ACE2 regulation under reduced oxygenation conditions remain elusive. To elucidate this aspect, brain pericytes were exposed to hypoxia as well as hypoxia/ischemia *in vitro*. Here we show that ACE2 expression significantly increased upon exposure to hypoxic and ischemic-like conditions (Fig. 7A). As hypoxia constitutes a pathological condition that persists in time within the tissues in various vascular-mediated brain disorders (Kisler et al., 2017), we evaluated the temporal expression profile of ACE2 in pericytes under normoxic and prolonged hypoxic conditions. We found that ACE2 protein expression remained significantly elevated 48 h, 72 h under hypoxic

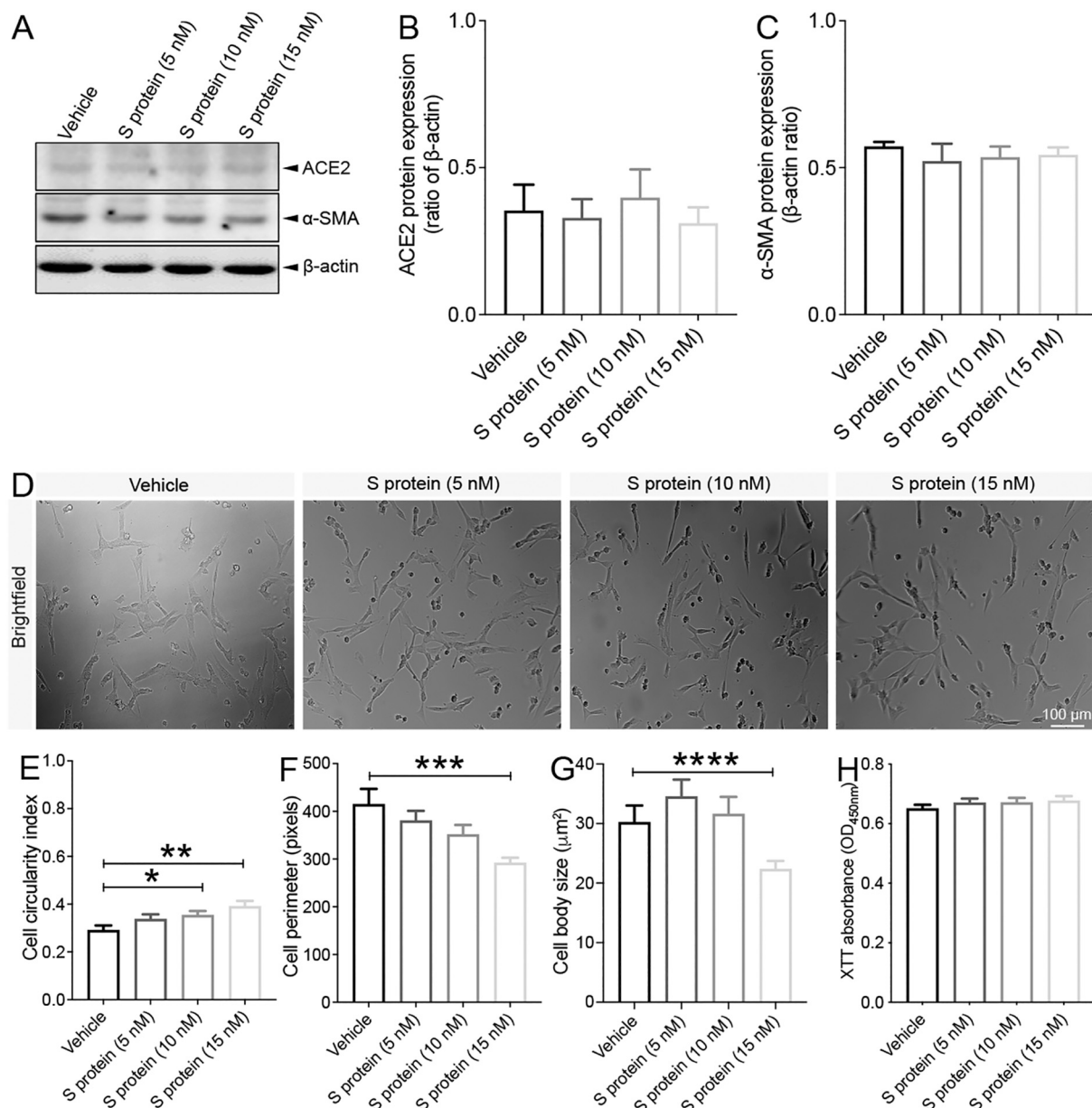


Fig. 5. S protein exposure does not influence the dynamics of VSMCs. **A)** Western blot analysis shows that **B)** ACE2 expression as well as **C)** α -SMA expression in human brain VSMCs remains unchanged 24 h after exposure to S protein. **D)** Brightfield images of living cells shows that the morphology of human VSMCs remains intact upon exposure to S protein for 24 h. **E)** Morphological analysis shows that cell circularity index slightly increases upon exposure of VSMCs to 10 nM and 15 nM S protein for 24 h. **F)** Cell perimeter slightly decreases only upon exposure to 15 nM S protein for 24 h. **G)** Cell body size slightly decreases only upon exposure to 15 nM S protein for 24 h. **H)** XTT cell viability assay shows that exposure to S protein for 24 h does not affect the survival of VSMCs. Data are mean \pm SEM ($n = 3$ independent experiments/ condition; Cell morphology analysis, $n =$ randomly selected 10 to 12 vehicle- and S protein-treated cells per image for a total of 3 images per experimental condition; XTT cell viability assay, $n = 12$ wells/ condition). * $P < 0.05$ / ** $P < 0.01$ / *** $P < 0.001$ / **** $P < 0.0001$ compared with vehicle-treated pericytes (two-tailed unpaired t-test). Vehicle, ddH₂O; XTT, 2/3-bis-(2-methoxy-4-nitro-5-sulphophenyl)-2H-tetrazolium-5-carboxanilide.

conditions (Fig. 7B). Next, we assessed whether hypoxia modulates S protein mediated ACE2 expression in pericytes. Our data indicate that ACE2 expression significantly increased following S protein stimulation for 24 h in pericytes exposed to hypoxia for 48 h (Fig. 7C). Immunofluorescence analysis indicated that ACE2 increased expression upon S protein exposure was accompanied by an enhanced localization to the cellular membrane, which was potentiated under hypoxic conditions (Fig. 7D). These results demonstrate that ACE2 expression in human brain pericytes is dynamic and is potently induced following exposure to S protein as well as under conditions in which oxygen levels are low.

3.7. Hypoxia modulates S protein mediated pericyte phenotypic transition

The vascular-mediated symptoms associated to COVID-19 pathogenesis are associated to impaired cerebral blood perfusion as well as pro-fibrotic responses (Lee et al., 2021; Thakur et al., 2021; Matschke et al., 2020; Fraiman et al., 2020; Ellul et al., 2020). However, the impact of hypoxia combined to S protein exposure on pericyte contractile and myofibroblastic phenotype remains totally unknown. Interestingly, we showed that hypoxia for 48 h increased α -SMA expression, which was further induced upon S protein exposure for 24 h (Fig. 8A). On the other hand, our data indicate that hypoxia did not affect S protein-induced expression of fibronectin, while it stimulated its

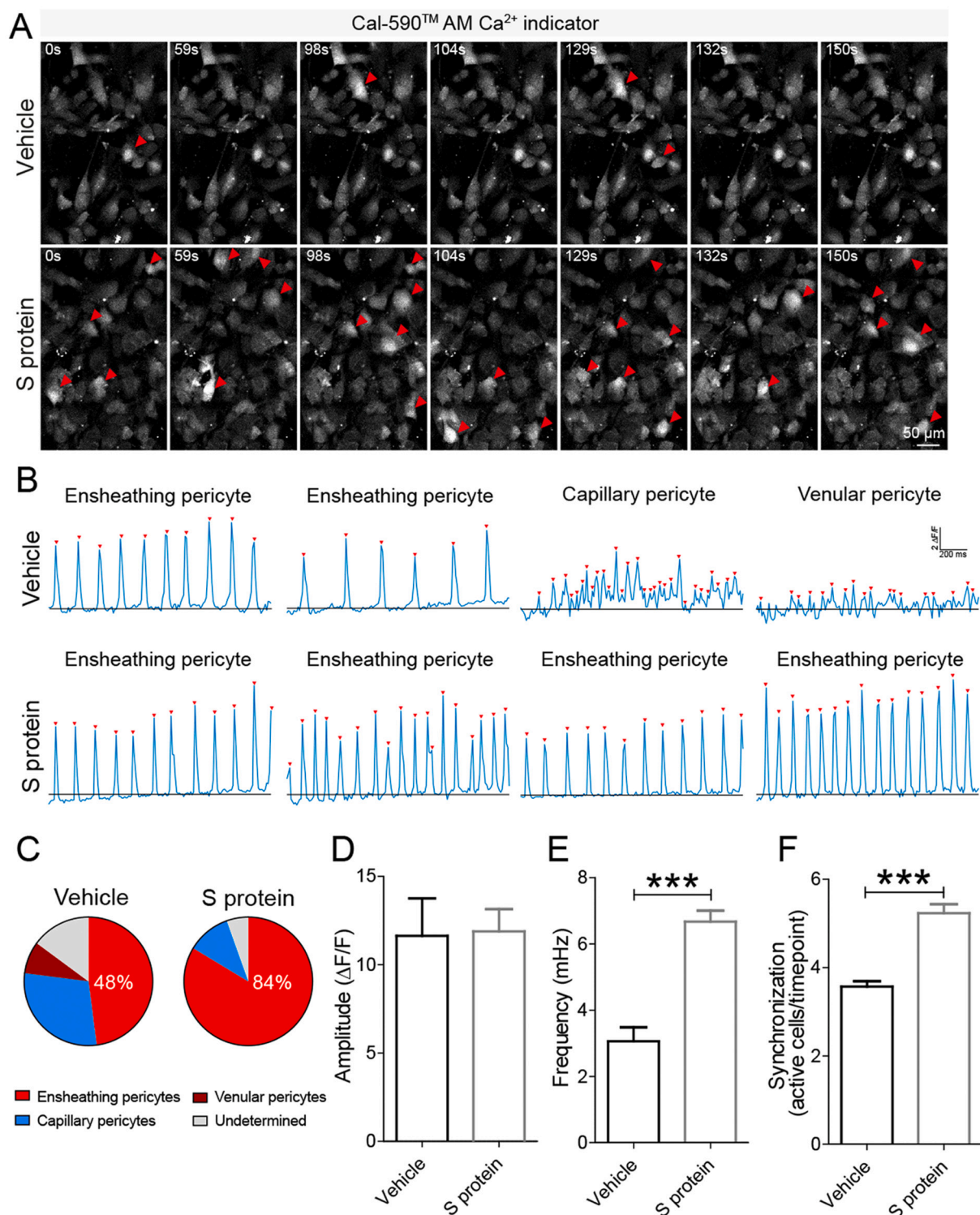


Fig. 6. S protein exposure modulates intracellular Ca²⁺ dynamics in pericytes. >A) Time-lapse imaging of Ca²⁺ dynamics in human brain vascular pericytes cultures using laser scanning confocal microscopy revealed that exposure to 10 nM S protein increases Ca²⁺ activity (white arrowheads). B) Representative traces of Ca²⁺ oscillatory activity showing that upon S protein exposure, pericytes adopt a distinct signature associated with the phenotype of ensheathing brain pericytes. Ca²⁺ events are marked by red arrowheads and blackline indicate the basal Ca²⁺ level. Note, distinct Ca²⁺ signatures in different types of human brain vascular pericytes, with the ensheathing phenotype associated with highly regular oscillatory Ca²⁺ events. C) Analysis of Ca²⁺ oscillatory activity indicates that S protein promoted an ensheathing pericyte phenotype. D) The amplitude of Ca²⁺ events remains unchanged in brain pericytes after exposure to S protein. E) Sharp increase in the frequency of Ca²⁺ events in brain pericytes upon exposure to S protein. F) Analysis of synchronized activity of Ca²⁺ events showing a strong increase in the level of synchronization in brain pericytes upon S protein exposure. Data are mean \pm SEM ($n = 7$ videos from 4 wells for 371 cells in vehicle-treated brain pericytes / $n = 6$ videos from 4 wells for 382 cells in S protein-treated cells). *** $P < 0.001$ compared with vehicle-treated pericytes (two-tailed unpaired t-test). (For interpretation of the references to colour in this figure legend, the reader is referred to the web version of this article.)

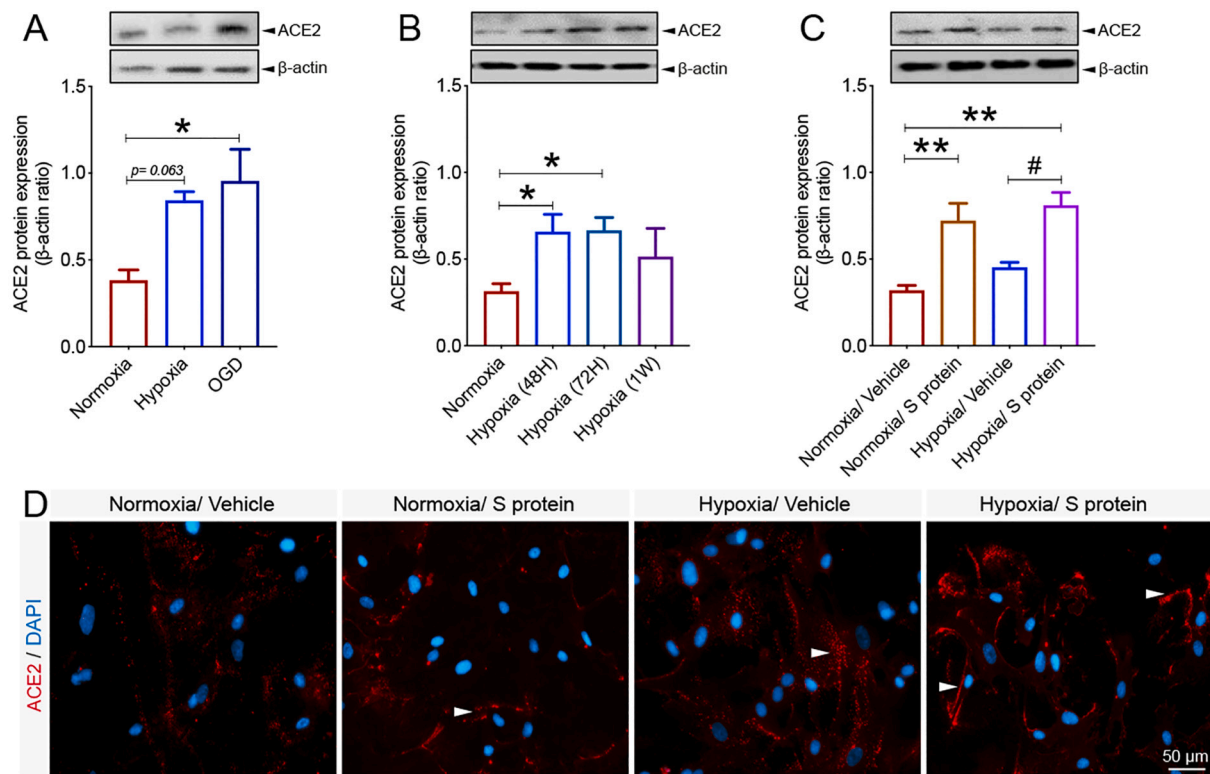


Fig. 7. Hypoxic/ischemic conditions modulate ACE2 expression pattern in pericytes. **A)** Western blot analysis shows that ACE2 expression in human brain vascular pericytes increases 24 h after exposure to hypoxic (hypoxia) or ischemic-like (OGD) conditions. **B)** Western blot analysis shows that ACE2 expression in brain pericytes continues to increase under prolonged hypoxic conditions to reach a peak at 1 week. **C)** Western blot analysis shows that ACE2 expression in response to 10 nM S protein exposure for 24 h is exacerbated in brain pericytes pre-exposed to hypoxic conditions. **D)** Representative images of immunofluorescence staining that illustrate ACE2 expression pattern in response to S protein exposure for 24 h in brain pericytes pre-exposed to hypoxic conditions, outlining a possible redistribution at the cell membrane (white arrowheads). Data are mean \pm SEM ($n = 3$ independent experiments/condition; XTT cell viability assay $n = 9$ –12 wells/condition). * $P < 0.05$ /** $P < 0.01$ compared with normoxia vehicle-treated pericytes, and # $P < 0.05$ compared with hypoxia vehicle-treated pericytes (one-way analysis of variance (ANOVA) followed by Bonferroni's multiple comparison post-hoc test). Vehicle, ddH₂O; OGD, oxygen and glucose deprivation; 48H, 48 hours; 72H, 72 hours; 1W, 1 week; XTT, 2/3-bis-(2-methoxy-4-nitro-5-sulphophenyl)-2H-tetrazolium-5-carboxanilide.

expression at a similar level under normoxic and hypoxic conditions (Fig. 8B). Our data suggest that hypoxia increased NOTCH3 expression in brain pericytes, which was slightly augmented upon exposure to S protein (Fig. 8C). Additionally, we found that hypoxia for 48 h potently increased collagen I expression, which was induced in pericytes after 24 h of stimulation with S protein (Fig. 8D, E), which has been shown to play major role in various tissue fibrosis (Fernández-Klett et al., 2013; Dias and Göritz, 2018). The results suggest that hypoxia exacerbates S protein-mediated pericyte transition towards a contractile and myofibroblastic phenotype.

3.8. Exposure to S protein triggers oxidative stress in brain pericytes

COVID-19 pathogenesis is associated to cerebrovascular dysfunction and coagulopathies (Klok et al., 2020; Richardson et al., 2020; Thakur et al., 2021; Fraiman et al., 2020; Ellul et al., 2020), including the formation of ischemic and hypoxic lesions. Hypoxia/ischemia-induced oxidative and nitrosative stress have been shown to induce pericytes sustained pathological contraction (Yemisci et al., 2009). Yet, the impact of S protein on oxidative stress in pericytes remains totally unknown. Here we found that stimulation with S protein at 10 nM for 24 h under hypoxic conditions compromised pericyte viability, which was assessed using XTT assay (Fig. 9A). S protein exposure for 24 h, independently of hypoxia, induced lipid peroxidation associated to oxidative stress in pericytes (Fig. 9B). Additionally, our data indicate that hypoxia exacerbated the S protein-mediated generation of ROS and RNS in brain pericytes (Fig. 9C). Hypoxia exacerbated total ROS generation upon

exposure of brain pericytes to S protein (Fig. 9D). However, S protein did not affect superoxide generation in brain pericytes, whereas hypoxia did (Fig. 9E). Finally, NO production in brain pericytes upon S protein exposure was induced by hypoxia (Fig. 9F). The results thus demonstrate that S protein triggers oxidative and nitrosative stress in pericytes, a response that is exacerbated under hypoxic conditions.

3.9. S protein combined to hypoxia trigger an immune response in brain pericytes

As mentioned, pericytes have been shown to possess immune functions at the neurovascular interface (ElAli et al., 2014; Kisler et al., 2017; Török et al., 2021). It has been recently proposed that pericyte dysfunction upon infection with SARS-CoV-2 causes microvasculature inflammation and injury (He et al., 2020; Bocci et al., 2021). However, whether S protein is capable of eliciting pericyte immunoreactivity, which in turn mediate microvascular injury remains elusive. Here we show that S protein at 15 nM increased the ratio of p65-NF- κ B phosphorylation, as early as 6 h after stimulation (Fig. 10A), which remained elevated 24 h later (Fig. 10B). Importantly, our data indicate that hypoxia for 48 h significantly increased the ratio of p65-NF- κ B phosphorylation, which further augmented upon S protein stimulation for 24 h (Fig. 10C). Next, we profiled the expression pattern of cytokines and chemokines and found out that brain pericyte ubiquitously express various molecules implicated in modulating the immune response, namely stromal cell-derived factor (SDF)-1, intercellular adhesion molecule (ICAM), interleukin (IL)18, MIF, and plasminogen activator

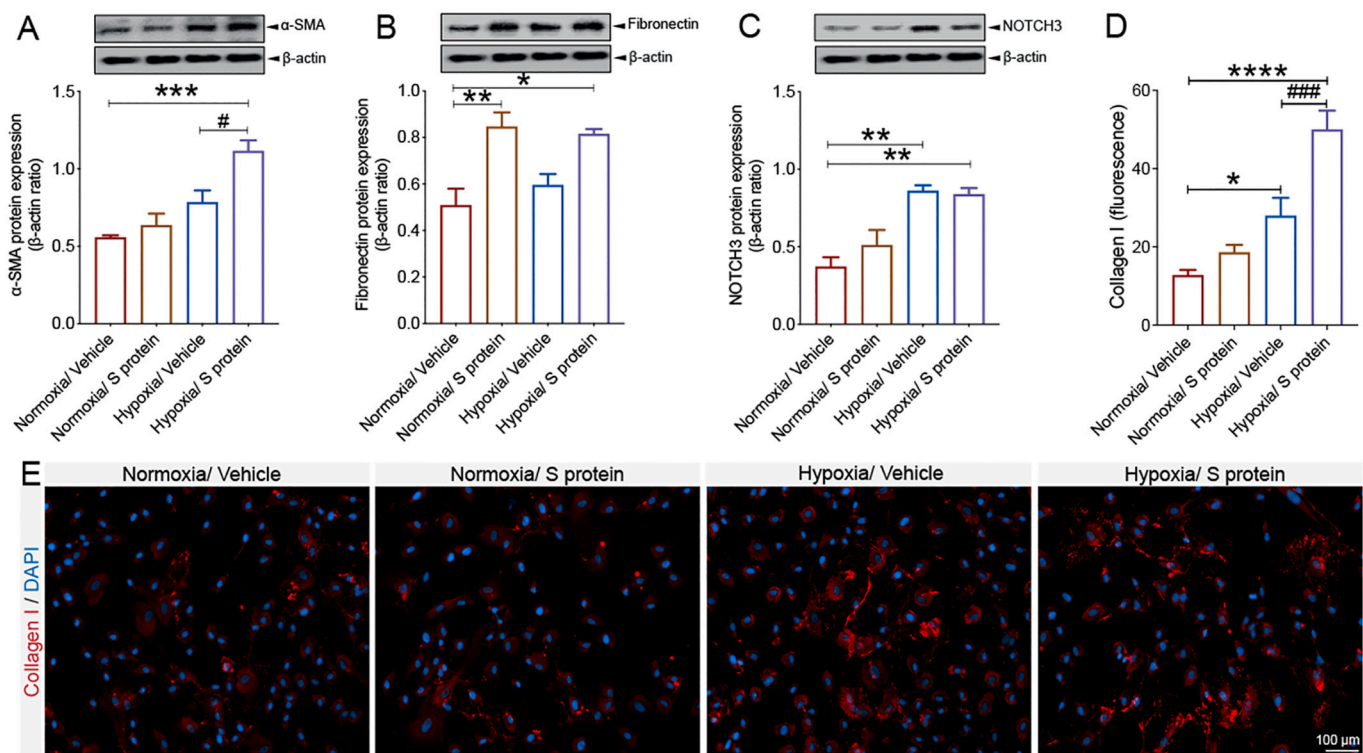


Fig. 8. S protein-mediated phenotypic changes in pericytes are modulated by hypoxia. **A)** Western blot analysis shows that α -SMA expression increases in brain pericytes pre-exposed to hypoxic conditions and is further induced upon exposure to S protein at 10 nM for 24 h. **B)** Western blot analysis shows that fibronectin expression increases in brain pericytes 24 h after exposure to S protein, independently of the hypoxic conditions. **C)** Western blot analysis shows that NOTCH3 expression increases upon exposure to S protein for 24 h and hypoxia, which does not influence S protein-mediated effects. **D)** Analysis of immunofluorescence intensity shows that expression of the pro-fibrotic protein collagen I increases following S protein exposure for 24 h in brain pericytes pre-exposed to hypoxic conditions. **E)** Representative images of immunofluorescence staining that illustrates the expression pattern of collagen I in brain pericytes pre-exposed to hypoxic conditions and exposed for 24 h to S protein. Data are mean \pm SEM ($n = 3$ independent experiments/condition). * $P < 0.05$ /** $P < 0.01$ /**** $P < 0.001$ /**** $P < 0.0001$ compared with normoxia vehicle-treated pericytes, and # $P < 0.05$ /### $P < 0.001$ compared with hypoxia vehicle-treated pericytes (one-way analysis of variance (ANOVA) followed by Bonferroni's multiple comparison post-hoc test). Vehicle, ddH₂O.

inhibitor (PAI)-1 (Fig. 10D). Importantly, our data suggest that among these molecules, MIF expression was potently increased in brain pericytes in response to hypoxia associated to 24 h exposure to S protein (Fig. 10E). The results suggest that S protein in presence of hypoxic conditions mediates pericyte immunoreactivity leading the production of cytokine and chemokines involved in immune cell trafficking within the vasculature.

3.10. Intranasal SARS-CoV-2 infection induces acute ischemic-like pericyte reactivity

As mentioned, COVID-19 pathogenesis is often accompanied by neurovascular complications, including focal and multifocal ischemic lesions (Lee et al., 2021; Thakur et al., 2021; Fraiman et al., 2020; Ellul et al., 2020). Moreover, our cell-based experiments have revealed that hypoxia upregulates ACE2 expression, which was further exacerbated upon S protein exposure. However, murine ACE2 does not recognize SARS-CoV-2 S protein, that is why K18-hACE2 transgenic mice expressing human ACE2 were used. We first verified the basal distribution of ACE2 in the brain of healthy C57BL6/J mice and found out that it is abundantly expressed in brain pericytes expressing desmin (Fig. 11A). We next assessed whether the SARS-CoV-2 intranasal infection could affect pericyte dynamics in the brain of mice like S protein effects *in vitro*. For this purpose, we compared the dynamics of PDGFR β^+ pericytes in the brain of C57BL6/J wildtype mice after ischemic stroke and in the brain of K18-hACE2 after SARS-CoV-2 intranasal infection. Our data indicate that pericytes were reactive in the brain of K18-hACE2 mice at 4 days after SARS-CoV-2 infection, translated by an increased

expression of PDGFR β , and exhibited close reactivity pattern to pericytes located at the ischemic brain of C57BL6/J wildtype mice (Fig. 11B). Moreover, we observed an increased ACE2 vascular expression in the brain of K18-hACE2 mice infected with SARS-CoV-2, which was comparable to its expression pattern in the ischemic brain of C57BL6/J wildtype mice (Fig. 11C). Moreover, we found out that S protein reached the brain of C57BL6/J wildtype mice 24 h after intranasal infusion, upon permeabilization of the nasal mucosa (Fig. 11D). Together, the results suggest that intranasal SARS-CoV-2 infection triggers an ischemic-like reactivity of ACE2 $^+$ PDGFR β^+ pericytes, presumably via S protein, thus potentially contributing to the pathobiology of cerebrovascular disorders observed in COVID-19.

4. Discussion

Infection of respiratory and gastrointestinal ACE2 $^+$ epithelial cells with SARS-CoV-2 accounts for the common typical symptoms in COVID-19 patients (Mao et al., 2020; Klok et al., 2020). Nonetheless, COVID-19 pathogenesis is often accompanied by neurological manifestations that are essentially linked to neurovascular complications, such as stroke and microangiopathies (Klok et al., 2020; Richardson et al., 2020; Thakur et al., 2021; Fraiman et al., 2020; Ellul et al., 2020). Accumulating evidence is suggesting that PDGFR β^+ pericytes constitute the main cell type at the neurovascular interface that abundantly expresses ACE2 (He et al., 2020; Bocci et al., 2021; Alison-Silva et al., 2013). Recently, a "COVID-19-pericyte hypothesis" was proposed as an attempt to understand the neurological manifestations associated with SARS-CoV-2 infection (He et al., 2020). It postulates that the passage of blood-

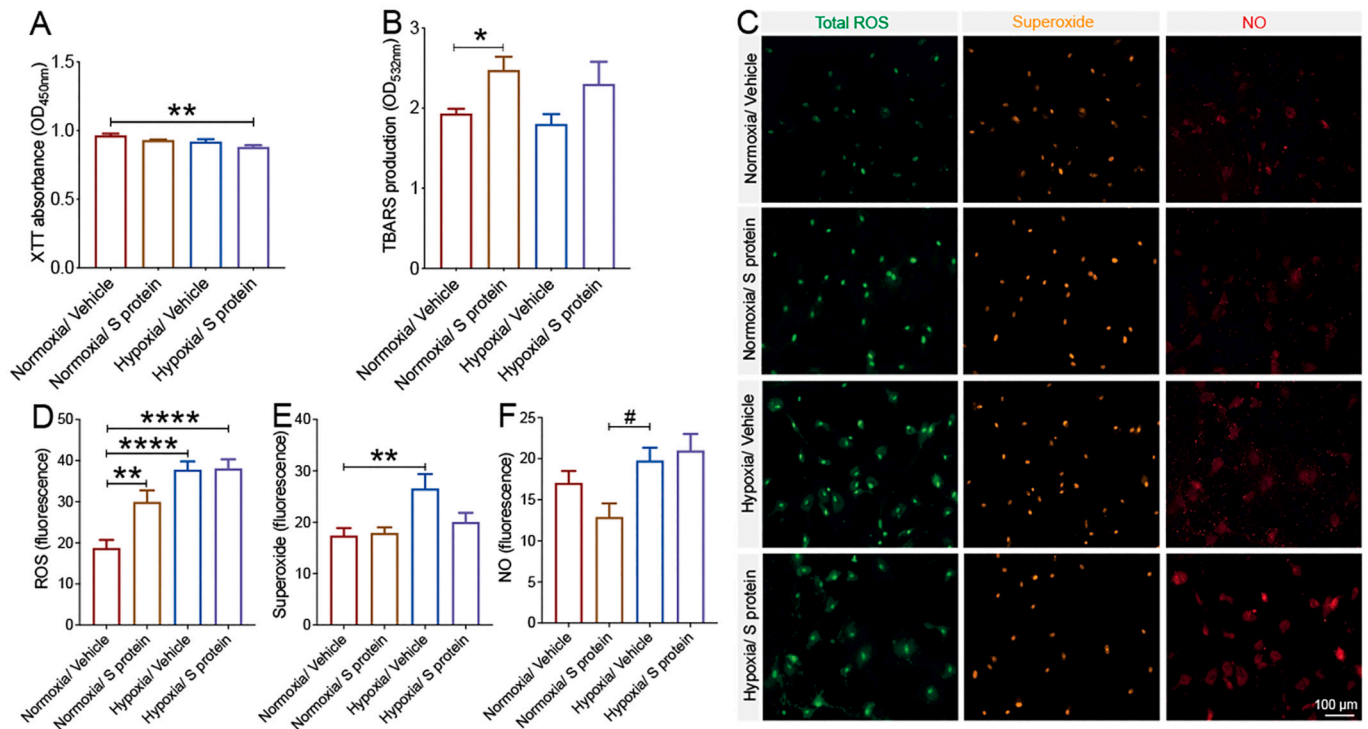


Fig. 9. S protein exposure causes oxidative and nitrosative stress in pericytes. A) XTT cell viability assay shows that pre-exposure to hypoxic conditions does not affect the survival of human brain vascular pericytes following exposure to 10 nM S protein for 24 h. B) TBARS assay shows that exposure of brain pericytes to S protein for 24 h increases lipid peroxidation independently upon the hypoxic conditions. C) Representative fluorescence images of ROS/RNS assay, which probes real time reactive oxygen and nitrogen species production by brain pericytes. D) Analysis of the fluorescence intensity shows that S protein exposure for 24 h induces total ROS generation in brain pericytes, a response that is exacerbated under hypoxic conditions. E) Analysis of the fluorescence intensity shows that hypoxia increases superoxide production in brain pericytes independently upon S protein. F) Analysis of the fluorescence intensity shows that S protein exposure for 24 h associated to hypoxia increases NO generation in brain pericytes. Data are mean \pm SEM ($n = 3$ independent experiments/ condition; ROS/RNS assay, $n =$ randomly selected 14 to 15 cells per well of 12-well plates). * $P < 0.05$ / ** $P < 0.01$ / **** $P < 0.0001$ compared with normoxia vehicle-treated pericytes, and # $P < 0.05$ compared with hypoxia vehicle-treated pericytes (one-way analysis of variance (ANOVA) followed by Bonferroni's multiple comparison post-hoc test). Vehicle, ddH₂O; XTT, 2/3-bis-(2-methoxy-4-nitro-5-sulphophenyl)-2H-tetrazolium-5-carboxanilide; ROS/RNS, reactive oxygen/nitrogen species.

derived SARS-CoV-2 across a permeable BBB infects perivascular pericytes, thus leading to microvasculature inflammation (He et al., 2020). Indeed, it has been shown that the virus could possibly reach the olfactory bulb and the brainstem, causing microvascular injuries (Lee et al., 2021; Thakur et al., 2021). Yet, it remains unclear whether a productive SARS-CoV-2 infection inside the brain is required to mediate the observed effects.

In this report, we unravelled previously undescribed effects of SARS-CoV-2 S protein in deregulating the vascular and immune functions of brain pericytes, which may account for vascular injuries underlying cerebrovascular events in COVID-19. Furthermore, we highlighted the role of hypoxia associated to vascular comorbidities, which aggravate COVID-19 pathogenesis, in exacerbating S protein-mediated effects on brain pericytes. More precisely, we have demonstrated that S protein increased ACE2 expression in human brain vascular pericytes in a dose-dependent manner. Moreover, S protein exposure induced the expression of contractile and myofibroblastic markers, namely α -SMA, fibronectin, NOTCH3, and collagen I, which was potentiated by hypoxia. These effects were accompanied by adoption of S protein-exposed brain pericytes to an elongated and contracted morphology. Moreover, we found that S protein exposure promoted a Ca²⁺ signature that is associated to contractile ensheathing pericytes, accompanied by highly regular oscillatory Ca²⁺ fluctuations. Moreover, S protein exposure induced lipid peroxidation, oxidative and nitrosative stress in pericytes, and activated the master regulator of inflammation, NF- κ B, via p65 phosphorylation. Importantly, S protein exposure accompanied by hypoxia increased the expression of MIF, a pro-inflammatory cytokine that plays a major role in modulating the immune response within the

vasculature (Stark et al., 2013). In K18-hACE2 transgenic mice, we found out that the intranasal infection with SARS-CoV-2 induced pericyte reactivity by increasing PDGFR β expression similarly as ischemic stroke. Moreover, SARS-CoV-2 intranasal infection potently induced ACE2 expression at the brain vasculature of K18-hACE2 transgenic mice, similarly as ischemic stroke. Finally, we observed that S protein released in the intranasal cavity could reach the brain of normal C57BL6/J mice following nasal mucosa permeabilization. Collectively, our results suggest that SARS-CoV-2 triggers via S protein the pathological reactivity of pericytes at the neurovascular interface (Fig. 12). This knowledge is critical to understand the mechanisms underlying the pathobiology of cerebrovascular disorders associated to COVID-19, and thereby to develop efficient therapies aiming to attenuate the neurovascular complications.

Although it is now well established that brain pericytes abundantly express ACE2, the dynamics of its expression following the exposure to SARS-CoV-2 S protein remains elusive. Here we show that ACE2 expression in brain human pericytes increases upon exposure to SARS-CoV-2 S protein, suggesting the presence of a positive regulatory mechanism that increases pericyte responsiveness to S protein. It has been shown that pericyte contraction induced by oxidative and nitrosative stress impairs brain perfusion via constriction of the brain microvasculature (Yemisci et al., 2009). Pericyte contraction was associated to elevated levels of cytoplasmic α -SMA implicated in cell contraction (Yemisci et al., 2009). Here we show that S protein exposure dose dependently induced profound morphological changes characterized by the emergence of a contracted profile in pericytes, as well as induced the expression of α -SMA, which was accompanied by an

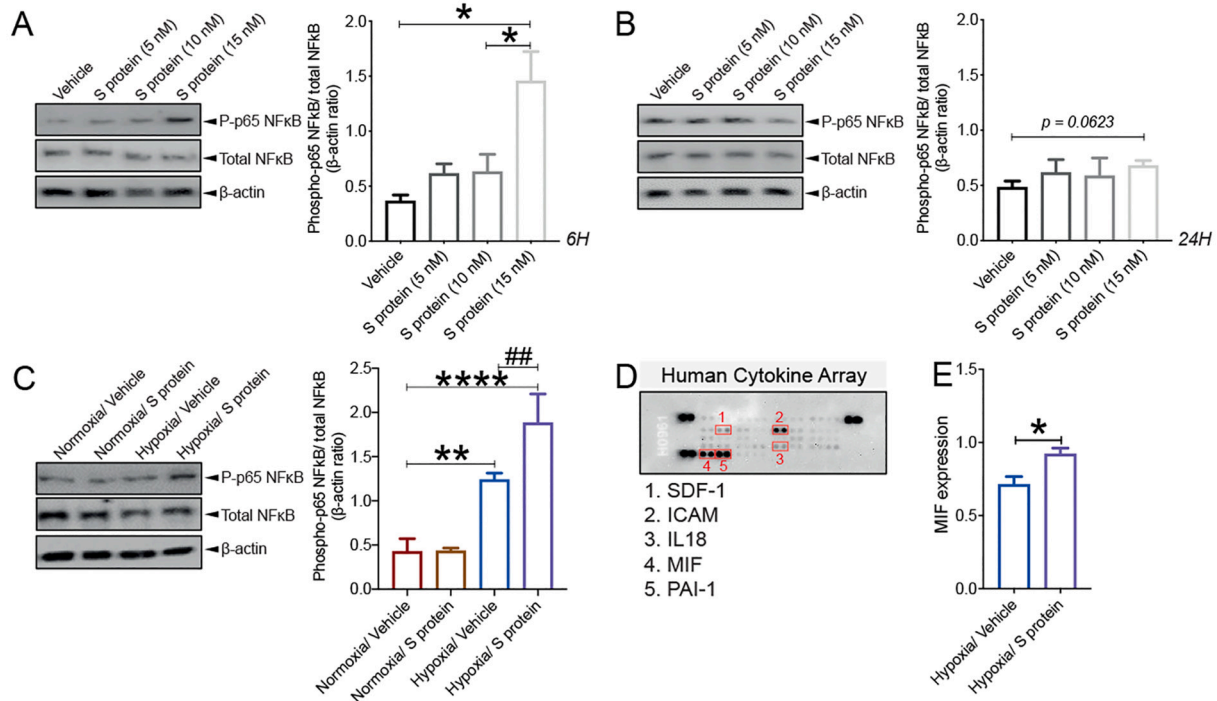


Fig. 10. S protein exposure induces a strong immune reaction in pericytes. **A)** Western blot analysis shows that the ratio of phosphorylated p65-NF-κB over total NF-κB (i.e pathway activation) increases in human brain vascular pericytes upon exposure to 15 nM S protein for 6 h. **B)** Western blot analysis shows that the ratio of phosphorylated p65-NF-κB over total NF-κB remains elevated upon exposure of brain pericytes to S protein for 24 h, without statistical significance. **C)** Western blot analysis shows that the ratio of phosphorylated p65-NF-κB over total NF-κB increases upon stimulation of brain pericytes pre-exposed to hypoxic conditions with S protein for 24 h. **D)** Representative images of the Proteome Profiler Human Cytokine Array membranes showing that brain pericytes ubiquitously express various immune mediators, including stromal cell-derived factor (SDF)-1, intercellular adhesion molecule (ICAM), interleukin (IL)18, MIF, and plasminogen activator inhibitor (PAI)-1. **E)** Analysis of the cytokine and chemokine array shows that MIF expression is increased in response to S protein exposure for 24 h in brain pericytes pre-exposed to hypoxic conditions. Data are mean ± SEM ($n = 3$ independent experiments/ condition; Proteome Profiler Human Cytokine Array, $n = 3$ pooled independent experiments/ condition). **(A-B)** $*P < 0.05$ compared with vehicle or S-protein-treated pericytes (two-tailed unpaired t-test); **(C)** $**P < 0.01$ / $****P < 0.0001$ compared with normoxia vehicle-treated pericytes, and $##P < 0.01$ compared with hypoxia vehicle-treated pericytes (one-way analysis of variance (ANOVA) followed by Bonferroni's multiple comparison post-hoc test); **(D)** $*P < 0.05$ compared with vehicle-treated pericytes (two-tailed unpaired t-test). Vehicle, ddH₂O.

increased expression of extracellular matrix proteins associated to fibrosis, namely fibronectin and collagen I. The pericyte-myofibroblast transition constitutes a critical pathological feature in tissue fibrosis in various pathologies (Di Carlo and Peduto, 2018). Under hypoxic and ischemic conditions, reactive pericytes are suggested to contribute to fibrotic scar formation, presumably via trans-differentiation into myofibroblast-like cells (Fernández-Klett et al., 2013). As such, our findings suggest that S protein exposure may facilitate the transition of pericytes towards a contractile and myofibrogenic phenotype, which may impair neurovascular functions. NOTCH3 plays an important role in brain vascular integrity, mainly by regulating pericyte survival and vascular coverage (Wang et al., 2014). NOTCH3 signaling impairment, such as aggregation of its ECD in brain pericytes wrapping brain vasculature caused by genetic mutations, has been shown to be directly involved in the pathobiology of cerebral autosomal dominant arteriopathy with subcortical infarcts and leukoencephalopathy (CADASIL) (Ghosh et al., 2015). Notwithstanding the above, the impact of S protein exposure on NOTCH3 regulation in human pericytes remains to be addressed. Here we show that S protein exposure increased NOTCH3 expression and protein aggregation in brain pericytes. More investigations are required to fully elucidate NOTCH3 dynamic upon S protein. However, our data suggest that S protein exposure may alter pericyte function via impairing NOTCH3 signaling by at least promoting protein pathological aggregation. Moreover, S protein exposure reduced the cell circularity index, outlining the acquisition of an elongated and contracted morphology. Interestingly, these effects were not observed in VSMCs exposed to S protein despite ACE2 expression. These results suggest that VSMCs better resist the S protein-mediated effects

presumably since they are highly differentiated in comparison to pericytes. Ca²⁺ signaling plays a major role in regulating brain pericyte contractile function (Halaidych et al., 2019; Hartmann et al., 2021). PDGFRβ⁺ brain pericyte populations, which are present at specific locations within the vascular network, exhibit distinct and specific Ca²⁺ signatures (Glück et al., 2021). Ensheathing pericytes located at the level of penetrating arterioles and pre-capillaries, exhibited a SMC-like Ca²⁺ dynamics, and were characterized by an important contractile potential and capacity to regulate the CBF (Glück et al., 2021). Here, we found that the induced expression of contractile and myofibrogenic markers upon S protein exposure strongly correlated with the increased frequency and synchronicity of intracellular Ca²⁺ in pericytes. Importantly, S protein exposure potently promoted the acquisition of an ensheathing pericyte Ca²⁺ signature. This in line with recent reports indicating that SARS-CoV-2 binding to ACE2 triggered pericyte-mediated angiotensin-evoked cerebral capillary constriction (Hirunpattarasilp et al., 2021). Furthermore, it has been reported that the gliovascular cells displayed a significant increase in Ca²⁺ during and after epileptic seizures, causing neurovascular dysfunction translated by a sustained constriction of the cerebral vasculature (Yemisici et al., 2009). Taken together, our results suggest that S protein mediates a phenotypic switch in pericytes by promoting the contractile and myofibrogenic properties associated with a modulation of Ca²⁺ signaling. Future studies are warranted to elucidate the mechanisms underlying S protein mediated Ca²⁺ signaling in pericytes.

Brain pericytes are key regulators of the immune responses at the neurovascular interface by relaying signals from the periphery to the brain (ElAli et al., 2014; Kisler et al., 2017; Armulik et al., 2011).

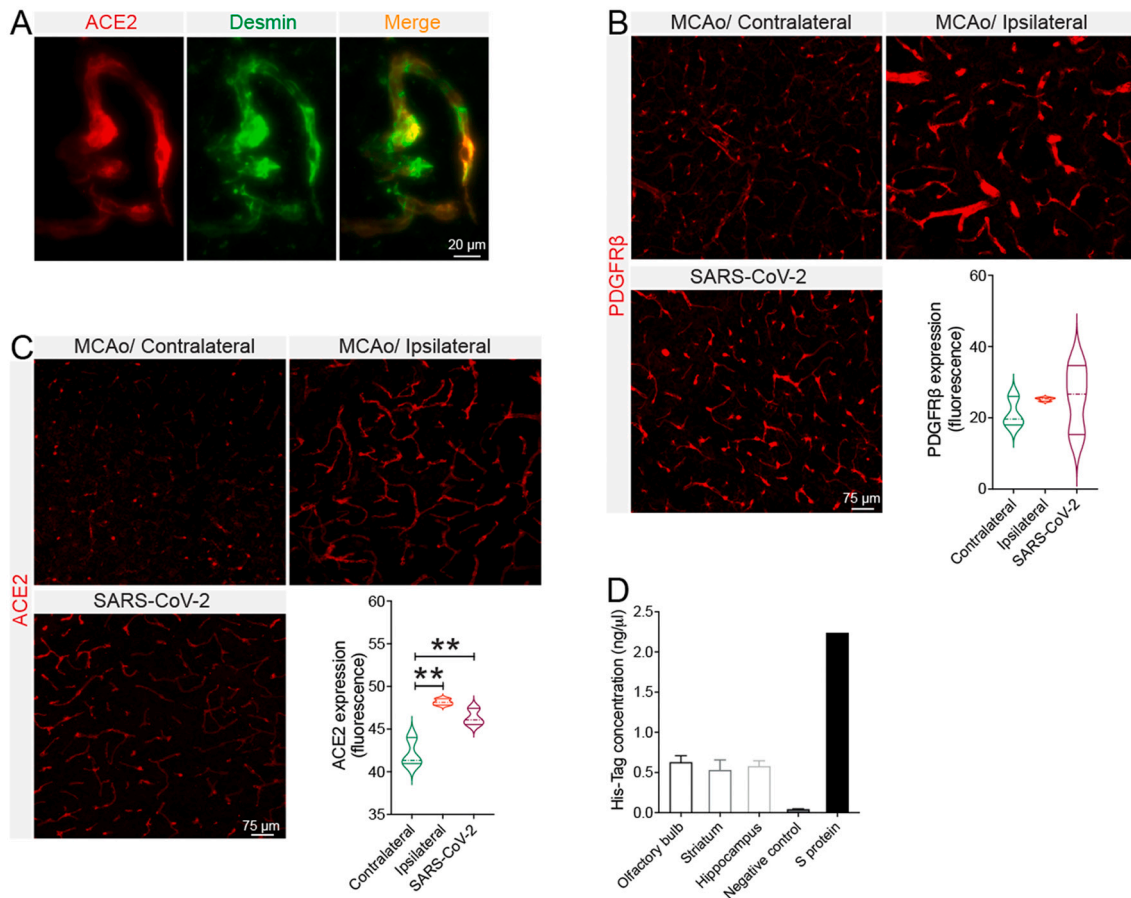


Fig. 11. SARS-CoV-2 intranasal infection induces pericyte reactivity in the brain. A) Representative images of immunofluorescence staining show that ACE2 (red) is co-localized with vascular pericytes labelled with desmin (green) in the brain of wildtype mice. B) Analysis of immunofluorescence intensity indicates that PDGFR β expression is induced in the brain of K18-hACE2 transgenic mice 4 days following intranasal infection with SARS-CoV-2, as well as in the ischemic ipsilateral hemisphere of C57BL6/J wildtype mice 3 days after cerebral ischemia induction via middle cerebral artery occlusion (MCAo). C) Analysis of immunofluorescence intensity indicates that ACE2 expression increases in the brain vasculature of K18-hACE2 transgenic mice 4 days following intranasal infection with SARS-CoV-2 as well as in the ischemic ipsilateral hemisphere of C57BL6/J wildtype mice 3 days after ischemic stroke. D) His-Tag ELISA analysis shows that the poly-histidine-tagged S protein is present in different brain regions 24 h after intranasal infusion. Data are mean \pm SEM ($n = 3$ animals/ condition). ** $P < 0.01$ compared with contralateral hemisphere (one-way analysis of variance (ANOVA) followed by Bonferroni's multiple comparison post-hoc test). (For interpretation of the references to colour in this figure legend, the reader is referred to the web version of this article.)

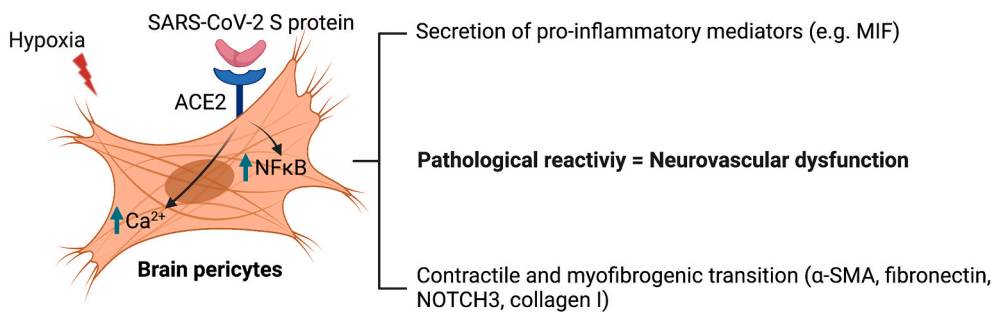


Fig. 12. Scheme illustrating the effects of S protein on brain pericytes in absence of productive viral infection. Exposure of ACE2⁺ human brain vascular pericytes to SARS-CoV-2 S protein active trimer induces NF- κ B signaling pathway and modulates intracellular Ca²⁺ activity. The intracellular signaling changes in brain pericytes upon S protein exposure are accompanied by an increased expression of contractile and myofibroblastic markers as well as secretion of inflammatory cytokines and chemokines. S protein effects are potentiated under hypoxic conditions, which are associated to vascular comorbidities that have been

demonstrated to exacerbate COVID-19 pathogenesis. We postulate that SARS-CoV-2 could impair neurovascular functions by deregulating the functions of ACE2⁺ pericytes via S protein active trimer.

Pericytes contribute to neuroimmunomodulation via secretion of immune-active molecules, adoption of macrophage-like activity, presentation of antigens, and regulation of leukocyte trafficking across the cerebral vasculature (ElAli et al., 2014; Török et al., 2021). Brain pericytes express basal levels of several cytokines and chemokines (Stark et al., 2013). Under inflammatory conditions, pericytes respond to the

immune challenge by increasing the expression of inflammatory mediators, including ROS and NO (Kovac et al., 2011). Moreover, α -SMA⁺ pericytes were demonstrated to detect danger signals, triggering pro-inflammatory profile, which was associated to an increased expression of MIF (Stark et al., 2013). Importantly, MIF production promoted the survival and migration of leukocytes within the vascularized tissue

(Stark et al., 2013). Previous findings indicated that activation of NF- κ B signaling pathway, a master regulator of inflammation, is crucially implicated in regulating the immune responses of brain pericytes (Guijarro-Muñoz et al., 2014; Rustenhoven et al., 2016). Interestingly, here we show that S protein exposure activated NF- κ B signaling pathway, which was accompanied by an enhanced expression of MIF. Our data indicate that S protein-mediated pericyte immunoreactivity may be implicated in exacerbating microvascular inflammation in COVID-19. The presence of vascular comorbid and risk factors, such as diabetes, hypertension, and obesity, in patients is now well established as an aggravating condition for COVID-19 pathogenesis (Richardson et al., 2020; He et al., 2020). These factors predispose for vascular injuries associated to pericyte dysfunction (ElAli et al., 2014; Armulik et al., 2011), which jointly contribute to the formation of local hypoxic and ischemic conditions. As such, we evaluated the impact of hypoxia on S protein effects on brain pericytes. Our findings indicate that ACE2 expression as well as S protein mediated effects on pericyte contractile and myofibroblastic transition were potently exacerbated under hypoxic conditions. Moreover, hypoxia significantly increased S protein-mediated NF- κ B signaling pathway activation as well as the expression of immune mediators. Our data suggest that the impact of hypoxia in individuals with vascular risk factors may aggravate the vascular-mediated neurological conditions associated to COVID-19.

Finally, we were interested in evaluating the dynamics of brain pericytes in response to SARS-CoV-2 infection. Interestingly, hypoxic, and hemorrhagic lesions were detected in the post-mortem brain of patients following SARS-CoV-2 infection (Lee et al., 2021; Thakur et al., 2021; Matschke et al., 2020). Hypoxia associated to ischemic stroke triggers a pathological reactivity and prolonged contraction of pericytes, leading to vascular constriction and CBF impairment, thus worsening injury (Yemisci et al., 2009). Here we show that SARS-CoV-2 intranasal infection induced an ischemic-like PDGFR β ⁺ pericyte reactivity in the brain of K18-hACE2 transgenic mice. Moreover, ACE2 vascular expression significantly increased in the brain of hACE2 mice intranasally infected with SARS-CoV-2, replicating the effects of ischemic insult. It has been previously shown that K18-hACE2 mice infected with SARS-CoV-2 exhibited encephalitis associated with inflamed meningeal vessels, extravasation of immune cells into the brain parenchyma, and microglial activation (Winkler et al., 2020). Our study indicates that SARS-CoV-2 infection induces the reactivity of PDGFR β ⁺ pericytes in the brain of these mice. It is noteworthy to mention that S protein infused in the intranasal cavity of normal C57BL6/J wildtype mice reached the brain when the nasal mucosal barrier was permeabilized using hyaluronidase. In this regard, pathogens, such as viruses, can disrupt the nasal epithelium barrier via the secretion of several proteases that degrade the extracellular matrix proteins (Zhang et al., 2016). SARS-CoV-2 infection has been shown to deregulate the structure of the nasal mucosal barrier (Gallo et al., 2021). Taken together, these observations indicate that deregulation of nasal mucosa ACE2⁺ cells upon SARS-CoV-2 infection might allow the entry of S protein accumulated in the intranasal cavity into the brain, possibility acting on ACE2⁺ pericytes. However, more investigations are required to characterize the neuropathological consequences of SARS-CoV-2 S protein mediated brain pericyte reactivity *in vivo*.

5. Conclusion

Our study indicates that SARS-CoV-2 S protein deregulates the vascular and immune functions of brain pericytes, thus providing new mechanistic insights into the pathobiology of cerebrovascular disorders associated to COVID-19. Moreover, our findings suggest that deregulation of pericytes upon SARS-CoV-2 infection through S protein could act upstream on the cascade of events leading to microangiopathies. It is important to mention here that our reported observations do not reflect or translate in any way the impact of S protein-based mRNA vaccines on brain pericytes, which have been proven to be safe. Indeed, S protein is

locally produced in the muscle cells upon mRNA translation within the injection site, and mRNA is rapidly cleared. Besides, our cell-based assays translate an exaggerated and prolonged exposure to S protein, thus better reflecting a severe nasopharyngeal infection with SARS-CoV-2. Our study suggests that targeting S protein interaction with brain pericytes may allow alleviating some of the vascular-mediated neurological conditions in COVID-19.

Supplementary data to this article can be found online at <https://doi.org/10.1016/j.nbd.2021.105561>.

Author statement

All authors have read and approved the final version of the manuscript. The authors declare no conflict of interest and contributed to the study as follow; RKM performed and analyzed the *in vitro* experiments and drafted the paper; NA, AF, AS performed and analyzed the Ca²⁺ imaging experiments; ASP assisted in performing the *in vitro* experiments; SL, MB and DMC performed the *in vivo* experiments; AS edited and finalized the draft; LF provided the SARS-CoV-2 infected brains and edited the text; AEA conceptualized the study, analyzed data, drafted, edited, and finalized the manuscript. The authors declare that the research was conducted in the absence of any commercial or financial relationships that could be construed as a potential conflict of interest.

Author contributions

The authors contributed to the study as follow; RKM performed and analyzed the *in vitro* experiments and drafted the paper; NA, AF, AS performed and analyzed the Ca²⁺ imaging experiments; ASP assisted in performing the *in vitro* experiments; SL, MB and DMC performed the *in vivo* experiments; AS edited and finalized the draft; LF provided the SARS-CoV-2 infected brains and edited the text; AEA conceptualized the study, analyzed data, drafted, edited, and finalized the manuscript. The authors declare that the research was conducted in the absence of any commercial or financial relationships that could be construed as a potential conflict of interest.

Acknowledgements

This work is supported by grants from the Neuroscience Thematic Research Center (CTRN) (#DR127915), the Natural Sciences and Engineering Research Council of Canada (NSERC) (#RGPIN-2017-06119), the Fonds de recherche du Québec - Santé (FRQS) (#35170), and the Canadian Institutes of Health Research (CIHR) (#169062) (all to AEA), and CIHR (#172632 to LF). RKM is supported by a postdoctoral fellowship from CIHR (# 164700). AEA holds a Tier 2 Canada Research Chair in molecular and cellular neurovascular interactions. We thank Dr. Daniel Manrique-Castano for assisting in the immunofluorescence analysis. We thank the *Laboratoire de Santé Publique du Québec* for providing the SARS-CoV-2 isolate used in this study.

References

- Alisson-Silva, F., Freire-de-Lima, L., Donadio, J.L., Lucena, M.C., Penha, L., Sá-Diniz, J. N., et al., 2013. Increase of O-glycosylated oncofetal fibronectin in high glucose-induced epithelial-mesenchymal transition of cultured human epithelial cells. *PLoS One* 8, e60471. <https://doi.org/10.1371/journal.pone.0060471>.
- Armulik, A., Genové, G., Betsholtz, C., 2011. Pericytes: developmental, physiological, and pathological perspectives, problems, and promises. *Dev. Cell* 21, 193–215. <https://doi.org/10.1016/j.devcel.2011.07.001>.
- Bocci, M., Oudenaarden, C., Sáenz-Sardà, X., Simrén, J., Edén, A., Sjölund, J., et al., 2021. Infection of brain pericytes underlying neuropathology of COVID-19 patients. *bioRxiv*. <https://doi.org/10.1101/2021.05.24.445532>.
- Burduga, T., Borysova, L., 2014. Calcium signalling in pericytes. *J. Vasc. Res.* 51, 190–199. <https://doi.org/10.1159/000362687>.
- Di Carlo, S.E., Peduto, L., 2018. The perivascular origin of pathological fibroblasts. *J. Clin. Invest.* 128, 54–63. <https://doi.org/10.1172/JCI93558>.
- Dias, D.O., Görizt, C., 2018. Fibrotic scarring following lesions to the central nervous system. *Matrix Biol.* 68–69, 561–570. <https://doi.org/10.1016/j.matbio.2018.02.009>.

- Dias, D.O., Kalkitsas, J., Kelahmetoglu, Y., Estrada, C.P., Tatarishvili, J., Holl, D., et al., 2021. Pericyte-derived fibrotic scarring is conserved across diverse central nervous system lesions. *Nat. Commun.* 12, 5501. <https://doi.org/10.1038/s41467-021-25585-5>.
- Doepfner, T.R., Ewert, T.A., Tönges, L., Herz, J., Zechariah, A., ElAli, A., et al., 2012. Transduction of neural precursor cells with TAT-heat shock protein 70 chaperone: therapeutic potential against ischemic stroke after intrastriatal and systemic transplantation. *Stem Cells* 30, 1297–1310. <https://doi.org/10.1002/stem.1098>.
- Dosch, S.F., Mahajan, S.D., Collins, A.R., 2009. SARS coronavirus spike protein-induced innate immune response occurs via activation of the NF-kappaB pathway in human monocyte macrophages in vitro. *Virus Res.* 142, 19–27. <https://doi.org/10.1016/j.virusres.2009.01.005>.
- ElAli, A., Thériault, P., Rivest, S., 2014. The role of pericytes in neurovascular unit remodeling in brain disorders. *Int. J. Mol. Sci.* 15, 6453–6474. <https://doi.org/10.3390/ijms15046453>.
- Ellul, M.A., Benjamin, L., Singh, B., Lant, S., Michael, B.D., Easton, A., et al., 2020. Neurological associations of COVID-19. *Lancet Neurol.* 19, 767–783. [https://doi.org/10.1016/S1474-4422\(20\)30221-0](https://doi.org/10.1016/S1474-4422(20)30221-0).
- Fernández-Klett, F., Potas, J.R., Hilpert, D., Blazek, K., Radke, J., Huck, J., et al., 2013. Early loss of pericytes and perivascular stromal cell-induced scar formation after stroke. *J. Cereb. Blood Flow Metab.* 33, 428–439. <https://doi.org/10.1038/jcbfm.2012.187>.
- Fraiman, P., Godeiro Junior, C., Moro, E., Cavallieri, F., Zedde, M., 2020. COVID-19 and cerebrovascular diseases: a systematic review and perspectives for stroke management. *Front. Neurol.* 11, 574694. <https://doi.org/10.3389/fneur.2020.574694>.
- Gallo, O., Locatello, L.G., Mazzoni, A., Novelli, L., Annunziato, F., 2021. The central role of the nasal microenvironment in the transmission, modulation, and clinical progression of SARS-CoV-2 infection. *Mucosal Immunol.* 14, 305–316. <https://doi.org/10.1038/s41385-020-00359-2>.
- Gengatharan, A., Malvaut, S., Marymonchik, A., Ghareghani, M., Snapyan, M., Fischer-Sternjak, J., et al., 2021. Adult neural stem cell activation in mice is regulated by the day/night cycle and intracellular calcium dynamics. *Cell* 184, 709–722.e13. <https://doi.org/10.1016/j.cell.2020.12.026>.
- Ghosh, M., Balbi, M., Hellal, F., Dichgans, M., Lindauer, U., Plesnila, N., 2015. Pericytes are involved in the pathogenesis of cerebral autosomal dominant arteriopathy with subcortical infarcts and leukoencephalopathy. *Ann. Neurol.* 78, 887–900. <https://doi.org/10.1002/ana.24512>.
- Glück, C., Ferrari, K.D., Binini, N., Keller, A., Saab, A.S., Stobart, J.L., Weber, B., 2021. Distinct signatures of calcium activity in brain mural cells. *Elife* 10, e70591. <https://doi.org/10.7554/eLife.70591>.
- Guijarro-Muñoz, I., Compte, M., Álvarez-Cienfuegos, A., Álvarez-Vallina, L., Sanz, L., 2014. Lipopolysaccharide activates Toll-like receptor 4 (TLR4)-mediated NF-κB signaling pathway and proinflammatory response in human pericytes. *J. Biol. Chem.* 289, 2457–2468. <https://doi.org/10.1074/jbc.M113.521161>.
- Halaidech, O.V., Mummery, C.L., Orlova, V.V., 2019. Quantifying Ca²⁺ signaling and contraction in vascular pericytes and smooth muscle cells. *Biochem. Biophys. Res. Commun.* 513, 112–118. <https://doi.org/10.1016/j.bbrc.2019.03.143>.
- Hartmann, D.A., Berthiaume, A.A., Grant, R.L., Harrill, S.A., Koski, T., Tieu, T., et al., 2021. Brain capillary pericytes exert a substantial but slow influence on blood flow. *Nat. Neurosci.* 24, 633–645. <https://doi.org/10.1038/s41593-020-00793-2>.
- He, L., Mäe, M.A., Muhl, L., Sun, Y., Pietilä, R., Nahar, K., et al., 2020. Pericyte-specific vascular expression of SARS-CoV-2 receptor ACE2 – implications for microvascular inflammation and hypercoagulopathy in COVID-19. *bioRxiv*. <https://doi.org/10.1101/2020.05.11.088500>.
- Hirunpattarasilp, C., James, G., Freitas, F., Sethi, H., Kittler, J.T., Huo, J., et al., 2021. SARS-CoV-2 binding to ACE2 triggers pericyte-mediated angiotensin-evoked cerebral capillary constriction. *bioRxiv*. <https://doi.org/10.1101/2021.04.01.438122>.
- Hoffmann, M., Kleine-Weber, H., Schroeder, S., Krüger, N., Herrler, T., Erichsen, S., et al., 2020. SARS-CoV-2 cell entry depends on ACE2 and TMPRSS2 and is blocked by a clinically proven protease inhibitor. *Cell* 181, 271–280.e8. <https://doi.org/10.1016/j.cell.2020.02.052>.
- Jean LeBlanc, N., Guruswamy, R., ElAli, A., 2018. Vascular endothelial growth factor isoform-B stimulates neurovascular repair after ischemic stroke by promoting the function of pericytes via vascular endothelial growth factor receptor-1. *Mol. Neurobiol.* 55, 3611–3626. <https://doi.org/10.1007/s12035-017-0478-6>.
- Jean LeBlanc, N., Menet, R., Picard, K., Parent, G., Tremblay, M.E., ElAli, A., 2019. Canonical Wnt pathway maintains blood-brain barrier integrity upon ischemic stroke and its activation ameliorates tissue plasminogen activator therapy. *Mol. Neurobiol.* 56, 6521–6538. <https://doi.org/10.1007/s12035-019-1539-9>.
- Kisler, K., Nelson, A.R., Montagne, A., Zlokovic, B.V., 2017. Cerebral blood flow regulation and neurovascular dysfunction in Alzheimer disease. *Nat. Rev. Neurosci.* 18, 419–434. <https://doi.org/10.1038/nrn.2017.48>.
- Klok, F.A., Kruip, M.J.H.A., van der Meer, N.J.M., Arbous, M.S., Gommers, D.A.M.P.J., Kant, K.M., et al., 2020. Incidence of thrombotic complications in critically ill ICU patients with COVID-19. *Thromb. Res.* 191, 145–147. <https://doi.org/10.1016/j.thromres.2020.04.013>.
- Kovac, A., Erickson, M.A., Banks, W.A., 2011. Brain microvascular pericytes are immunoreactive in culture: cytokine, chemokine, nitric oxide, and LRP-1 expression in response to lipopolysaccharide. *J. Neuroinflammation* 8, 139. <https://doi.org/10.1186/1742-2094-8-139>.
- Laredo, F., Plebanski, J., Tedeschi, A., 2019. Pericytes: problems and promises for CNS repair. *Front. Cell. Neurosci.* 13, 546. <https://doi.org/10.3389/fncel.2019.00546>.
- Lee, M.H., Perl, D.P., Nair, G., Li, W., Maric, D., Murray, H., et al., 2021. Microvascular injury in the brains of patients with Covid-19. *N. Engl. J. Med.* 384, 481–483. <https://doi.org/10.1056/NEJMc2033369>.
- Lovren, F., Pan, Y., Quan, A., Teoh, H., Wang, G., Shukla, P.C., et al., 2008. Angiotensin converting enzyme-2 confers endothelial protection and attenuates atherosclerosis. *Am. J. Physiol. Heart Circ. Physiol.* 295, H1377–H1384. <https://doi.org/10.1152/ajpheart.00331.2008>.
- Malvaut, S., Gribaudo, S., Hardy, D., David, L.S., Daroles, L., Labrecque, S., et al., 2017. CaMKII α expression defines two functionally distinct populations of granule cells involved in different types of odor behavior. *Curr. Biol.* 27, 3315–3329.e6. <https://doi.org/10.1016/j.cub.2017.09.058>.
- Mao, L., Jin, H., Wang, M., Hu, Y., Chen, S., He, Q., et al., 2020. Neurologic manifestations of hospitalized patients with coronavirus disease 2019 in Wuhan, China. *JAMA Neurol.* 77, 683–690. <https://doi.org/10.1001/jamaneurol.2020.1127>.
- Matschke, J., Lütgehetmann, M., Hagel, C., Spherhake, J.P., Schröder, A.S., Edler, C., et al., 2020. Neuropathology of patients with COVID-19 in Germany: a post-mortem case series. *Lancet Neurol.* 19, 919–929. [https://doi.org/10.1016/S1474-4422\(20\)30308-2](https://doi.org/10.1016/S1474-4422(20)30308-2).
- Menet, R., Bourassa, P., Calon, F., ElAli, A., 2020. DICKKOPF-related protein-1 inhibition attenuates amyloid-beta pathology associated to Alzheimer's disease. *Neurochem. Int.* 141, 104881. <https://doi.org/10.1016/j.neuint.2020.104881>.
- Oladunni, F.S., Park, J.G., Pino, P.A., Gonzalez, O., Akhter, A., Allué-Guardia, A., et al., 2020. Lethality of SARS-CoV-2 infection in K18 human angiotensin-converting enzyme 2 transgenic mice. *Nat. Commun.* 11, 6122. <https://doi.org/10.1038/s41467-020-19891-7>.
- Ou, X., Liu, Y., Lei, X., Li, P., Mi, D., Ren, L., et al., 2020. Characterization of spike glycoprotein of SARS-CoV-2 on virus entry and its immune cross-reactivity with SARS-CoV. *Nat. Commun.* 11, 1620. <https://doi.org/10.1038/s41467-020-15562-9>.
- Padhi, A., Singh, K., Franco-Barraza, J., Marston, D.J., Cukierman, E., Hahn, K.M., et al., 2020. Force-exerting perpendicular lateral protrusions in fibroblastic cell contraction. *Commun. Biol.* 3, 390. <https://doi.org/10.1038/s42003-020-01117-7>.
- Richardson, S., Hirsch, J.S., Narasimhan, M., Crawford, J.M., McGinn, T., Davidson, K.W., et al., 2020. Presenting characteristics, comorbidities, and outcomes among 5700 patients hospitalized with COVID-19 in the New York City area. *JAMA* 323, 2052–2059. <https://doi.org/10.1001/jama.2020.6775>.
- Ropa, J., Cooper, S., Capitano, M.L., Van't Hof, W., Broxmeyer, H.E., 2021. Human hematopoietic stem, progenitor, and immune cells respond ex vivo to SARS-CoV-2 spike protein. *Stem Cell Rev. Rep.* 17, 253–265. <https://doi.org/10.1007/s12015-020-10056-z>.
- Rustenhoven, J., Aalderink, M., Scotter, E.L., Oldfield, R.L., Bergin, P.S., Mee, E.W., et al., 2016. TGF- β 1 regulates human brain pericyte inflammatory processes involved in neurovascular function. *J. Neuroinflammation* 13, 37. <https://doi.org/10.1186/s12974-016-0503-0>.
- Stark, K., Eckart, A., Haidari, S., Tirniceriu, A., Lorenz, M., von Brühl, M.L., et al., 2013. Capillary and arteriolar pericytes attract innate leukocytes exiting through venules and 'instruct' them with pattern-recognition and motility programs. *Nat. Immunol.* 14, 41–51. <https://doi.org/10.1038/ni.2477>.
- Sweeney, M.D., Zhao, Z., Montagne, A., Nelson, A.R., 2019. Zlokovic BV (2019) blood-brain barrier: from physiology to disease and back. *Physiol. Rev.* 99, 21–78. <https://doi.org/10.1152/physrev.00050.2017>.
- Thakur, K.T., Miller, E.H., Glendinning, M.D., Al-Dalahmah, O., Banu, M.A., Boehme, A.K., et al., 2021. COVID-19 neuropathology at Columbia University Irving Medical Center/New York Presbyterian Hospital. *Brain*. <https://doi.org/10.1093/brain/awab148>.
- Tischbirek, C.H., Birkner, A., Konnerth, A., 2017. In vivo deep two-photon imaging of neural circuits with the fluorescent Ca²⁺ indicator Cal-590. *J. Physiol.* 595, 3097–3105. <https://doi.org/10.1113/JP272790>.
- Török, O., Schreiner, B., Schaffnerath, J., Tsai, H.C., Maheshwari, U., Stifter, S.A., et al., 2021. Pericytes regulate vascular immune homeostasis in the CNS. *Proc. Natl. Acad. Sci. U. S. A.* 118, e2016587118. <https://doi.org/10.1073/pnas.2016587118>.
- Wang, Y., Pan, L., Moens, C.B., Appel, B., 2014. Notch3 establishes brain vascular integrity by regulating pericyte number. *Development* 141, 307–317. <https://doi.org/10.1242/dev.096107>.
- Wang, L., Sievert, D., Clark, A.E., Lee, S., Federman, H., Gastfriend, B.D., et al., 2021. A human three-dimensional neural-perivascular 'assembloid' promotes astrocytic development and enables modeling of SARS-CoV-2 neuropathology. *Nat. Med.* 27, 1600–1606. <https://doi.org/10.1038/s41591-021-01443-1>.
- Winkler, E.S., Bailey, A.L., Kafai, N.M., Nair, S., McCune, B.T., Yu, J., et al., 2020. SARS-CoV-2 infection of human ACE2-transgenic mice causes severe lung inflammation and impaired function. *Nat. Immunol.* 21, 1327–1335. <https://doi.org/10.1038/s41590-020-0778-2>.
- Yemisci, M., Gursoy-Ozdemir, Y., Vural, A., Can, A., Topalkara, K., Dalkara, T., 2009. Pericyte contraction induced by oxidative-nitrosative stress impairs capillary reflow despite successful opening of an occluded cerebral artery. *Nat. Med.* 15, 1031–1037. <https://doi.org/10.1038/nm.2022>.
- Zhang, N., Van Crombrugge, K., Gevaert, E., Bachert, C., 2016. Barrier function of the nasal mucosa in health and type-2 biased airway diseases. *Allergy* 71, 295–307. <https://doi.org/10.1111/all.12809>.
- Zhou, P., Yang, X.L., Wang, X.G., Hu, B., Zhang, L., Zhang, W., et al., 2020. A pneumonia outbreak associated with a new coronavirus of probable bat origin. *Nature* 579, 270–273. <https://doi.org/10.1038/s41586-020-2012-7>.